Amino Acid Residues That Influence the Binding of Manganese or Calcium to Photosystem II. 2. The Carboxy-Terminal Domain of the D1 Polypeptide†

Hsiu-An Chu, Anh P. Nguyen, and Richard J. Debus*

Department of Biochemistry, University of California at Riverside, Riverside, California 92521-0129

Received November 1, 1994; Revised Manuscript Received February 22, 1995⊗

ABSTRACT: To identify amino acid residues that ligate the manganese and calcium ions of photosystem II or are otherwise crucial to water oxidation, site-directed mutations were constructed in the unicellular cyanobacterium *Synechocystis* sp. PCC 6803 at all conserved carboxylate and histidine residues in the carboxy-terminal domain of the D1 polypeptide. Mutants with impaired photoautotrophic growth or oxygen evolution were characterized *in vivo* by measuring changes in the yield of variable chlorophyll *a* fluorescence after a saturating flash or brief illumination given in the presence of an electron-transfer inhibitor or following each in a series of saturating flashes given in the absence of inhibitor [Chu, H.-A., Nguyen, A. P., & Debus, R. J. (1994) *Biochemistry 33*, 6137−6149]. Mutants were also characterized after propagation in media having other cations substituted for calcium. We conclude that His-332, Glu-333, His-337, and Asp-342 influence the assembly and/or stability of the manganese cluster, that His-332, Glu-333, and His-337 may ligate manganese, that Asp-342 may ligate manganese, calcium, or both, that Glu-333 and Asp-342 may play important structural roles, and that His-332, Glu-333, and His-337 influence the binding of calcium, although Glu-333 is unlikely to ligate Ca^{2+} directly. Several His-332, Glu-333, His-337, and Asp-342 mutants were very light sensitive, possibly because toxic activated oxygen species were released from altered or partly assembled manganese clusters. Finally, mutations at Asp-342 do not prevent posttranslational cleavage of the carboxy-terminal extension of the D1 polypeptide's precursor form *in vivo*.

In the preceding paper in this issue (Chu et al., 1995), we described the characterization of site-directed photosystem II (PSII)[1] mutants having substitutions in the lumenal interhelical domains of the D1 polypeptide. These characterizations, undertaken to identify amino acid residues that ligate the Mn and Ca^{2+} ions of the oxygen-evolving complex, were conducted *in vivo* by noninvasive methods based on chlorophyll *a* fluorescence (Chu et al., 1994a). They confirmed that Asp-170 is a possible ligand of Mn and showed that His-190 is a possible ligand of Mn and that Asp-59 and Asp-61 are possible ligands of Ca^{2+}. In this paper, we present the results of our *in vivo* characterizations of mutants having substitutions in the D1 polypeptide's carboxy-terminal region. This region extends from approximately Ser-291 to the carboxy-terminal residue of the mature polypeptide, Ala-344. The data presented will guide future studies of isolated mutant PSII particles to residues of particular interest and to mutants that contain the most stable or most efficiently assembled oxygen-evolving complexes.

† This work was funded by the National Institutes of Health (GM 43496).

* Author to whom correspondence should be addressed.

⊗ Abstract published in *Advance ACS Abstracts,* April 15, 1995.

[1] Abbreviations: bp, base pair; Chl, chlorophyll *a*; DCBQ, 2,6-dichloro-*p*-benzoquinone; DCMU, 3-(3,4-dichlorophenyl)-1,1-dimethylurea; F_{eq}, steady-state fluorescence yield produced by weak monitoring flashes in the presence of DCMU; MES, 2-morpholinoethanesulfonic acid; P_{680}, primary chlorophyll electron donor; PSII, photosystem II; Q_A, primary plastoquinone electron acceptor; Q_B, secondary plastoquinone electron acceptor; S_n, oxidation state of the oxygen-evolving complex with *n* oxidizing equivalents stored; wild-type*, control *Synechocystis* strain constructed in the same manner as site-directed mutants, but with no mutation; Y_Z, rapid electron donor to P_{680}^+ (Tyr-161 of the D1 polypeptide); Y_D, slow electron donor to P_{680}^+ (Tyr-160 of the D2 polypeptide).

MATERIALS AND METHODS

All mutants except H337F were constructed in the *psb*A-2 gene of *Synechocystis* sp. PCC 6803 as described previously (Chu et al., 1994b). The H337F mutant was obtained as a spontaneous pseudorevertant of H337V cells. The wild-type* strain was the same as that described in the preceding paper (Chu et al., 1995). The identity of each mutant, the absence of unwanted mutations, and the innocence of silent mutations introduced to create sites for restriction endonucleases were verified as described previously (Chu et al., 1994a,b, 1995), except that transformations performed to verify the absence of unwanted mutations outside the *psb*A-2 gene employed the 403-bp *Sau*3AI/*Sau*3AI fragment, which includes the TAA "stop" codon. Cells were propagated at light intensities of 50−60 (normal light) or 5−6 μE m^{-2} s^{-1} (dim light), as indicated, and were prepared for analysis as described previously and in the preceding paper (Chu et al., 1994a, 1995). Measurements of light-saturated rates of oxygen evolution and chlorophyll *a* fluorescence were performed as described previously (Chu et al., 1994a, 1995), the latter with a modified Walz (Effeltrich, Germany) pulse−amplitude−modulation fluorometer. The fluorescence yield elicited by the monitoring flashes in the presence of DCMU rose rapidly from an initial level, F_0, to a steady-state level that we denote F_{eq} (Chu et al., 1994a, 1995). The kinetics of the decay of fluorescence yield after flash or continuous illumination in the presence of DCMU were analyzed using Jandel Scientific's (San Rafael, CA) PeakFit program, version 3.18. Unless stated otherwise, three exponentially decaying components were assumed (fewer components yielded nonrandom residuals). The relative PSII content of cells on a chlorophyll basis was estimated from the total yield

0006-2960/95/0434-5859$09.00/0

of variable chlorophyll *a* fluorescence ($F_{max} - F_0$) measured in the presence of DCMU and hydroxylamine (Philbrick et al., 1991; Nixon & Diner, 1992; Nixon et al., 1992; Chu et al., 1994a, 1995). Measurements were performed as described previously (Chu et al., 1994a). In a previous study of 21 mutants, including 10 described in this paper, the relative PSII contents estimated in this manner correlated well with those estimated from [^{14}C]DCMU binding studies (Chu et al., 1994a). Nevertheless, we will refer to the fluorescence-based estimates as "apparent" PSII contents.

RESULTS AND DISCUSSION

The carboxy-terminal domain of the D1 polypeptide contains five conserved carboxylate residues and two conserved histidine residues (Svensson et al., 1991). Each was individually replaced with at least one residue having different chemical/ligation properties and, if possible, with one having similar properties. To minimize the possibility of long-range structural changes, the original residues were replaced with residues of similar size.

The following mutations caused no discernible effect on either photoautotrophic growth or oxygen evolution: D308N, D319N, D319E, E329Q, and E329D. We conclude that neither Asp-308, Asp-319, nor Glu-329 is crucial to photosynthetic water oxidation under the conditions of our experiments. The reasons for the absolute conservation of these residues in all known sequences of the D1 polypeptide from cyanobacteria, algae, and higher plants (Svensson et al., 1991) remain unknown. No further characterizations of these mutants were undertaken. In contrast, all mutations constructed at His-332, Glu-333, His-337, and Asp-342 were deleterious to both photoautotrophic growth and oxygen evolution and were investigated further. A total of nine mutations were constructed at His-332, six at Glu-333, eight at His-337, and four at Asp-342. In addition, all four Asp-342 mutants were also constructed as double mutants, which contained a TAG stop codon in place of the TCT Ser-345 codon to prevent translation of the D1 polypeptide's carboxy-terminal extension.

The remainder of this Results and Discussion section is divided into four parts. Part I describes mutations constructed at His-332, part II describes mutations constructed at Glu-333, and parts III and IV describe mutations constructed at His-337 and Asp-342, respectively. In each part, the growth and fluorescence characteristics of the individual mutants are presented first, followed by an evaluation of the possible involvement of the wild-type residue in Mn or Ca^{2+} ligation or in other aspects of PSII function.

(I) His-332

(A) Growth, Oxygen Evolution Characteristics, and PSII Contents of Mutants. The following mutants were constructed: H332Q, H332N, H332D, H332E, H332K, H332R, H332S, H332L, and H332Y. All nine mutants required glucose for propagation, even in dim light (Table 1). When propagated in normal light, only H332Q cells evolved oxygen at significant rates (15% ± 4% compared to wild-type* cells), although some oxygen evolution was reproducibly detected in H332S cells (3% ± 1%). When propagated in dim light, the oxygen evolution rate of H332Q cells was unchanged, but the rate of H332S cells increased to 10% ± 1%. In both mutants, oxygen-evolving activity was lost rapidly in saturating light. When propagated in normal light, the apparent PSII contents of H332D and H332E cells were similar to that of wild-type* cells (Table 1), whereas those of all other His-332 mutants were depressed to some degree. When propagated in dim light, the apparent PSII contents of H332S, H332K, and H332R cells increased substantially (Table 1).

(B) Fluorescence Characteristics of Mutants. (i) Electron Transfer to Y_Z^{ox}. The fluorescence yields that followed each of four saturating flashes spaced 50 ms apart are shown in Figure 1 for the mutants H332Q, H332N, H332D, H332E, H332K, and H332R (the H332K and H332R cells were propagated in dim light). When propagated in dim light, the data of the H332S, H332L, and H332Y mutants (not shown) resembled those of H332N and H332R cells. In H332Q, H332N, and H332R cells (Figure 1A,B,F), the maximum fluorescence yield after the second and subsequent flashes was partly quenched. More extensive quenching was observed in H332D, H332E, and H332K cells (Figure 1C–E). Indeed, the progressive quenching observed in the H332E mutant resembled that in mutants that lack photooxidizable[2] Mn ions [*e.g.*, in the mutants D170A, D170N, and D170T (Chu et al., 1994a)]. In all of the His-332 mutants, the extent of quenching diminished as the spacing between the saturating flashes was increased, becoming negligible at flash spacings of 600–800 ms (not shown). These data show that the reduction of Y_Z^{ox} is slowed dramatically in all of the His-332 mutants: a considerable fraction of Y_Z^{ox} remains oxidized for at least 50 ms following each saturating flash (Chu et al., 1994a).

In each mutant except H332Q, significant amounts of Q_A^- remained reduced 50 ms after each flash (Figure 1). These amounts decreased as the spacing between the saturating flashes was increased (not shown), showing that the slowest components of electron transfer from Q_A^- to Q_B were slowed significantly in these mutants, especially in H332E and H332K cells. A similar slowing of this electron-transfer step was noted previously in several Asp-170 mutants (Chu et al., 1994a, 1995) and in the mutants D61A, E65Q, E65A, E189D, E189Q, and E189N (Chu et al., 1995). As noted in the preceding paper in this issue (Chu et al., 1995), other workers have noted that many treatments that alter the donor side of PSII also alter the properties of Q_A and/or Q_B [*e.g.*, see Krieger and Weis (1992), Krieger et al. (1993), Johnson et al. (1995), and references cited in Chu et al. (1994a)].

(ii) Charge Recombination between Q_A^- and PSII Electron Donors. The decay of fluorescence yield that followed a saturating flash given to H332Q, H332N, H332D, H332E, H332K, and H332R cells is shown in Figure 2A–F (the H332K and H332R cells were propagated in dim light). When propagated in dim light, the H332S mutant (not shown) exhibited data similar to those of H332Q cells, while the H332L and H332Y mutants (not shown) exhibited data similar to those of H332R cells. The amplitudes and rates of the decay components are presented in Table 1 in comparison to those of wild-type* cells. All of the His-332 mutants exhibited significant amounts of rapid decay kinetics that presumably corresponds to charge recombination between Q_A^- and Y_Z^{ox}. The lowest amounts of rapid decay

[2] We define "photooxidizable Mn ions" as Mn ions that are bound to PSII when actinic illumination begins and that are oxidized by Y_Z^{ox} with a half-time much shorter than that of charge recombination between Q_A^- and Y_Z^{ox}.

Table 1: Comparison of Wild-Type* (wt*) and His-332 Mutant Strains

strain	growth light intensity (μE m^{-2} s^{-1})	photoautotrophic growth[a]	O_2 evolution[b] (% of wt*)	apparent PSII content[c] (% of wt*)	kinetics of Q_A^- oxidation after a single flash[d] (%)	k^{-1} (s)	no. of cultures included in analyses
wild-type*	50−60	+	100	100	16 ± 4	0.10 ± 0.04	8
					43 ± 4	0.60 ± 0.13	
					41 ± 7	2.8 ± 0.4	
H332Q	50−60	−	15 ± 4	75 ± 8	47 ± 6	0.032 ± 0.005	5
					16 ± 4	0.57 ± 0.20	
					38 ± 4	3.2 ± 0.2	
H332S	5−6	−	10 ± 1	60 ± 2	42 ± 3	0.04 ± 0.01	3
					24 ± 3	0.65 ± 0.12	
					34 ± 3	2.6 ± 0.5	
	50−60	−	3 ± 1	43 ± 5	47 ± 7	0.05 ± 0.02	5
					26 ± 9	0.88 ± 0.36	
					26 ± 4	4.4 ± 1.7	
H332N	50−60	−	0	54 ± 9	55 ± 4	0.010 ± 0.003	6
					30 ± 4	0.16 ± 0.07	
					15 ± 1	5.4 ± 1.3	
H332D	50−60	−	0	107 ± 14	29 ± 2	0.012 ± 0.003	4
					56 ± 2	0.35 ± 0.03	
					16 ± 1	4.1 ± 0.6	
H332E	50−60	−	0	122 ± 6	71 ± 1	0.008 ± 0.002	3
					23 ± 2	0.070 ± 0.020	
					6.4 ± 1.1	7.9 ± 0.4	
H332K	5−6	−	0	59 ± 16	66 ± 2	0.008 ± 0.001	2
					24 ± 1	0.069 ± 0.017	
					10 ± 2	4.7 ± 0.4	
	50−60	−	0	38 ± 5	51 ± 6	0.035± 0.010	4
					25 ± 5	1.1 ± 0.5	
					24 ± 4	10 ± 3	
H332R	5−6	−	0−3	72 ± 2	60 ± 2	0.04 ± 0.01	2
					16 ± 1	0.80 ± 0.20	
					24 ± 2	9.6 ± 0.5	
	50−60	−	0	36 ± 2	34 ± 4	0.09 ± 0.01	3
					24 ± 11	1.3 ± 0.6	
					43 ± 14	8.6 ± 3.4	
H332L	5−6	−	0	37 ± 6	64 ± 5	0.015 ± 0.006	2
					20 ± 1	0.38 ± 0.23	
					16 ± 4	11 ± 1	
	50−60	−	0	33 ± 2	33 ± 8	0.05 ± 0.03	3
					22 ± 7	1.0 ± 0.15	
					44 ± 9	11 ± 4	
H332Y	5−6	−	0	28 ± 2	41 ± 10	0.05 ± 0.02	2
					33 ± 8	0.59 ± 0.17	
					26 ± 2	8.7 ± 0.5	
	50−60	−	0	25 ± 10	38 ± 2	0.17 ± 0.03	3
					21 ± 4	1.3 ± 0.2	
					40 ± 7	11 ± 1	

[a] Measured in growth medium without glucose. [b] Initial rates measured in growth medium. The eight wild-type* cultures used in this study evolved 680 ± 30 μmol of O_2 (mg of Chl)$^{-1}$ h^{-1} (Chu et al., 1994a). [c] Estimated from the total yield of variable chlorophyll *a* fluorescence ($F_{max} - F_0$). For the H332Q, H332N, and H332L cells propagated at 50−60 μE m^{-2} s^{-1}, these estimates have been shown to correlate with those estimated from [^{14}C]DCMU binding studies (Chu et al., 1994a). For the other mutants and growth conditions listed, this correlation is assumed. [d] Measured in the presence of DCMU and analyzed by assuming three exponentially decaying components. The relative amplitude (%) and the inverse of the rate constant of each component are reported. See left panels of Figure 2.

(30−50%) were exhibited by H332Q, H332D, H332S, and H332Y cells (Figure 2A,C and Table 1). In contrast, approximately 94% of the decay in H332E cells (Figure 2D) and approximately 90% of the decay in H332K cells (Figure 2E) were rapid (*i.e.*, characterized by inverse rate constants of 70 ms or less).

The slower decaying components in H332Q and H332S cells resembled those in wild-type* cells. In the H332D mutant, one of the two slower components decayed more rapidly, and the other more slowly, than in wild-type* cells. Similar behavior was noted previously in the D170E mutant (Boerner et al., 1992; Chu et al., 1994a). In H332N, H332E, and H332K cells, the slowest decay components were somewhat slower than those in wild-type* cells. In all of these mutants, the two slower components presumably correspond to charge recombination between Q_A^- and an oxidized form of a multinuclear Mn cluster. The slowest decaying components in H332R, H332L, and H332Y cells exhibited inverse rate constants of 9−11 s, which are similar to the rates of the slowest components measured in cells that lack the extrinsic 33 kDa polypeptide (Chu et al., 1994b). These very slow decays could correspond to charge recombination between Q_A^- and either a single oxidized Mn^{3+} ion or a Mn cluster of unknown nuclearity (Chu et al., 1994b). In PSII reaction centers having an intact Mn cluster, the rate of charge recombination is determined by the equilibrium between S_2P_{680} and $S_1P_{680}^+$ (Bouges-Bocquet, 1980; Vass & Styring, 1991; Buser et al., 1992; Buser, 1993). If we assume that charge recombination between Q_A^- and P_{680}^+ is not altered by the mutations, the slowness of the slower

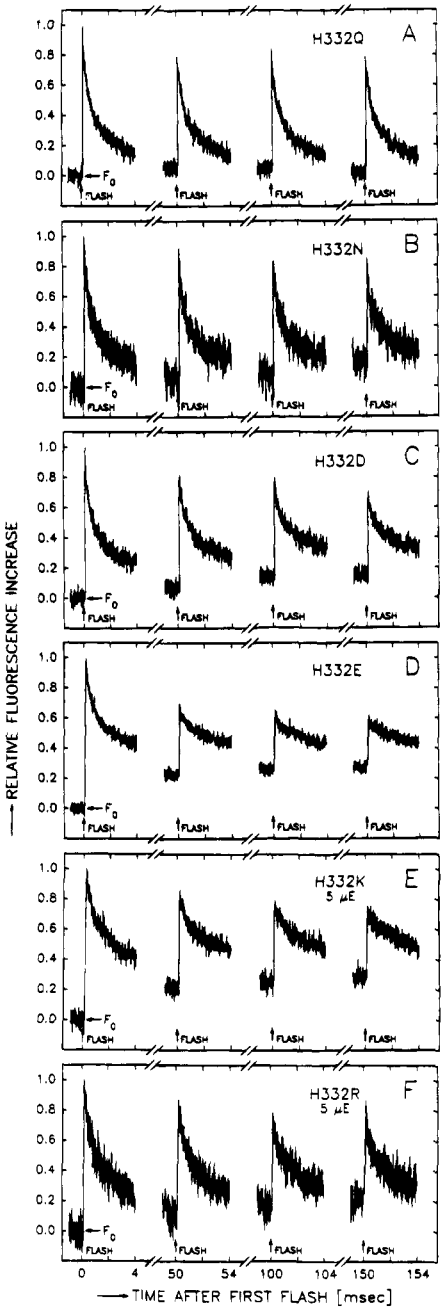

FIGURE 1: Yield of variable chlorophyll *a* fluorescence produced by each of four saturating flashes given at 50 ms intervals to His-332 mutant cells. Five milliseconds of data are shown for each flash. (A) H332Q; (B) H332N; (C) H332D; (D) H332E; (E) H332K; (F) H332R. The H332K and H332R cells were propagated in dim light (5−6 μE m^{-2} s^{-1}), as indicated. Conditions: 20 μg of Chl in 0.58 mL of 50 mM MES−NaOH, 25 mM $CaCl_2$, and 10 mM NaCl, pH 6.5, 22 °C. The cells were incubated in darkness for 1 min before the monitoring flashes were switched on. The frequency of the monitoring flashes was switched from 1.6 to 100 kHz for 5 ms beginning 1 ms before each saturating flash. The vertical scales are normalized to the maximum $(F - F_0)/F_0$ values measured after the first flash in each series. These values were 0.22 for (A), 0.12 for (B), 0.39 for (C), 0.45 for (D), 0.21 for (E), and 0.16 for (F). The data of H332S, H332L, and H332Y cells (not shown, propagated in dim light) resembled those of H332N and H332R, cells except that the maximum $(F - F_0)/F_0$ values were 0.34, 0.16, and 0.07, respectively. Four individual flash series were averaged for (A), four for (B), two each for (C) and (D), and five each for (E) and (F).

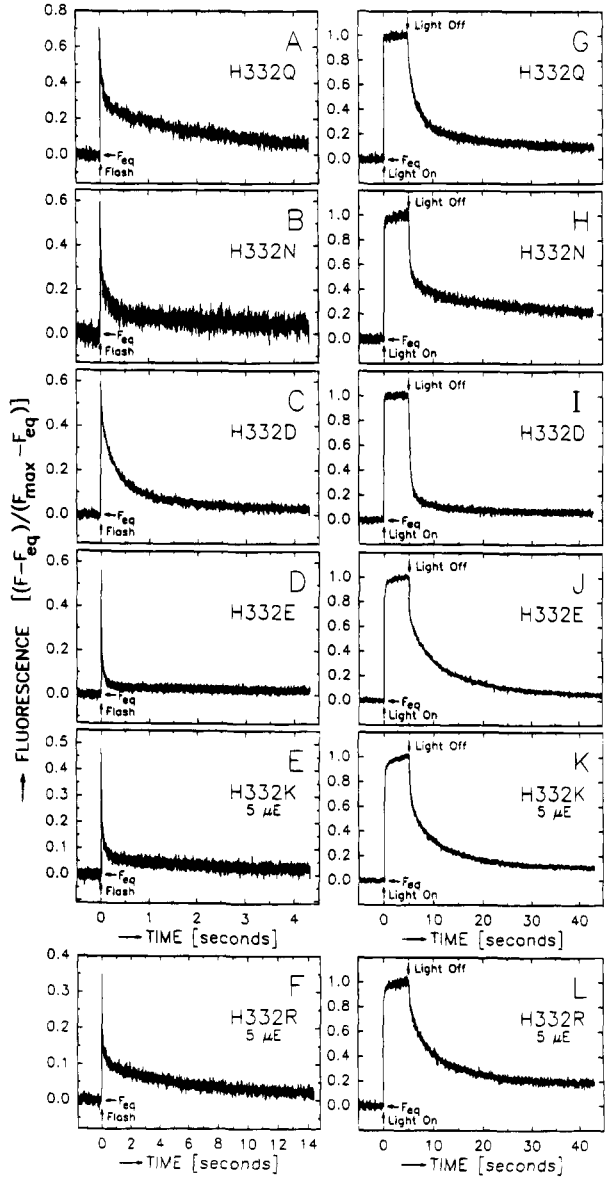

FIGURE 2: Formation and decay of Q_A^- in response to a saturating flash (left panels) or to 5 s of illumination (right panels) given to His-332 mutant cells in the presence of DCMU, as measured by changes in the yield of chlorophyll *a* fluorescence: (A, G) H332Q; (B, H) H332N; (C, I) H332D; (D, J) H332E; (E, K) H332K; (F, L) H332R. The H332K and H332R cells were propagated in dim light, as indicated. Note the three different time scales employed in this figure. The conditions were the same as in Figure 1 except that samples were incubated in darkness for 1 min in the presence of 0.3 mM *p*-benzoquinone and 1 mM potassium ferricyanide before DCMU was added to a concentration of 40 μM (the final concentration of ethanol was 2%). For a definition of F_{eq}, see Materials and Methods. The data in each left panel were normalized with the F_{max} value determined in the corresponding right panel. The F_{max} values (right panels) were not increased by the addition of hydroxylamine. The traces in (A) and (B) represent the computer average of 8 traces, while those in (C−F) represent the computer average of 13−16 traces. The monitoring flashes were applied at 1.6 kHz. The data of H332S cells (not shown, propagated in dim light) resembled those of H332Q cells, while the data of H332L and H332Y cells (not shown, propagated in dim light) resembled those of H332R cells.

decay components suggests that the oxidized forms of the Mn clusters in H332N, H332E, H332K, H332R, H332L, and H332Y cells are somewhat stabilized with respect to the S_2 state of the Mn cluster in wild-type* cells. Similar stabilization has been observed in cells that lack the extrinsic 33 kDa polypeptide (Philbrick et al., 1991; Vass et al., 1992; Burnap et al., 1992; Chu et al., 1994b). In contrast, the more rapid

decay of one of the two slower components in H332D cells suggests that the oxidized form of some of the Mn clusters in these cells is slightly *destabilized* with respect to the S_2 state in wild-type* cells.

The charge recombination kinetics of H332K, H332R, H332L, and H332Y cells slowed considerably when these mutants were propagated in normal light instead of dim light (Table 1). Indeed, the charge recombination kinetics of H332K, H332R, H332L, and H332Y cells propagated in *normal* light resembled those of mutant cells that lack the extrinsic 33 kDa polypeptide (Chu et al., 1994b). The charge recombination kinetics of H332S cells was also slowed when propagated in normal light, but to a lesser extent (Table 1). In addition to exhibiting altered charge recombination kinetics, H332K, H332R, and H332S cells exhibited lower apparent PSII contents when propagated in normal light (see above and Table 1). These results show that H332S, H332K, H332R, H332L, and H332Y cells are extremely light-sensitive. In contrast, H332Q, H332N, H332D, and H332E cells are *not* particularly light-sensitive, that is, they exhibited no significant changes in apparent PSII content or fluorescence properties when propagated in normal light instead of dim light (not shown).

In many of the His-332 mutants, the apparent rate of charge recombination between Q_A^- and Y_Z^{ox} was unusually rapid. In H332N, H332D, H332E, and H332K cells (the latter propagated in dim light), the rapid component of fluorescence yield decay exhibited an inverse rate constant of 8−12 ms (Table 1), compared to approximately 50 ms in D170H and D170R cells (Chu et al., 1994a). The observed rate of charge recombination between Q_A^- and Y_Z^{ox} is determined by the equilibrium between $Y_Z^{ox}P_{680}$ and $Y_ZP_{680}^+$ (Yerkes et al., 1983; Buser et al., 1990; Buser, 1993). By assuming that charge recombination between Q_A^- and P_{680}^+ is not altered by the mutations, these results imply that the Y_Z^{ox}/Y_Z midpoint potential increased slightly in the H332N, H332D, H332E, and H332K mutants, as concluded previously for D170A and D170S cells (Chu et al., 1994a, 1995). These results imply that His-332 may exert some influence on the redox properties of Y_Z.

(iii) Photoaccumulation of Q_A^-. To estimate the fractions of reaction centers that lack photooxidizable Mn ions in the His-332 mutants *in vivo*, cells were illuminated for 1−15 s in the presence of DCMU. The kinetics of Q_A^- oxidation in H332Q, H332N, H332D, H332E, H332K, and H332R cells after 5 s of illumination are presented in Figure 2G−L. The H332K and H332R cells were propagated in dim light. The data of H332S cells (propagated in dim light, not shown) resembled those of H332Q cells. The data of H332L and H332Y cells (propagated in dim light, not shown) resembled those of H332R cells. In all mutants, the rates of the two *faster* components of Q_A^- oxidation after 5 s of illumination (Figure 2G−L) were roughly similar to the rates of the two *slower* components observed after a single flash (Figure 2A−F and Table 1). Both components presumably correspond to charge recombination between Q_A^- and an oxidized form of a Mn cluster (Chu et al., 1994a). However, unlike in other mutants (Chu et al., 1994a), the amplitudes of these components were much smaller after a single flash than after 5 s of illumination (*e.g.*, compare Figure 2D,J for the H332E mutant and Figure 2E,K for the H332K mutant). The fraction of Q_A^- that *photoaccumulated* in each mutant during 5 s of illumination (*i.e.*, the fraction that oxidized

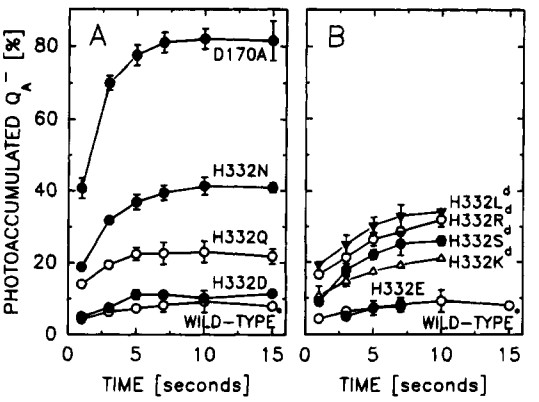

FIGURE 3: Fraction of PSII reaction centers in His-332 mutant cells that photoaccumulated Q_A^- after illumination for specific intervals of time. This fraction is defined as that fraction of reaction centers in which Q_A^- was oxidized with a time constant of 1−2 min (see Figure 2G−L and text). (A) Photoaccumulation of Q_A^- in H332D, H332Q, and H332N cells in comparison to wild-type* and D170A cells. (B) Photoaccumulation of Q_A^- in H332E, H332K, H332S, H332R, and H332L cells in comparison to wild-type* cells. The H332K, H332S, H332R, and H332L cells were propagated in dim light, as indicated by the superscript d. The data of H332Y cells (not shown, propagated in dim light) resembled those of H332L cells. The wild-type* and D170A data are taken from Chu et al. (1994a) to facilitate comparisons. The conditions were the same as in Figure 2.

slowly, with a time constant of 1−2 min) ranged from 7.2% ± 2.0% in H332E cells (Figure 2J) to 37% ± 2% in H332N cells (Figure 2H), compared to 7.2% ± 0.9% in wild-type* cells (Chu et al., 1994a). Figure 3A shows the fraction of Q_A^- that photoaccumulated during 1−15 s of illumination in H332D, H332Q, and H332N cells in comparison to that in wild-type* cells. Data for D170A cells, which lack photooxidizable Mn ions (Chu et al., 1994a), are shown for comparison. Figure 3B shows the corresponding data for H332E cells and for H332S, H332K, H332R, and H332L cells propagated in dim light. The data of H332Y cells propagated in dim light (not shown) overlapped those of H332L cells.

In all mutants except H332D and H332E, the rates of Q_A^- photoaccumulation were heterogeneous, with a fraction of PSII reaction centers photoaccumulating Q_A^- rapidly (generally during the first second of illumination), and other fractions photoaccumulating at much slower rates. These data imply that a considerable fraction of PSII reaction centers in all of the His-332 mutants except H332D and H332E lack photooxidizable Mn ions *in vivo*. By comparing the extent of Q_A^- photoaccumulation after 7−10 s of illumination with that in wild-type* and D170A cells, we estimate that 12−18% of H332K reaction centers, 16−19% of H332Q reaction centers, 22−25% of H332S reaction centers, 26−33% of H332R reaction centers, 32−36% of H332L and H332Y reaction centers, and 42−44% of H332N reaction centers lack photooxidizable Mn ions *in vivo*. In contrast, ≥95% of H332D reaction centers and essentially 100% of H332E reaction centers contain photooxidizable Mn clusters, albeit of unknown nuclearity. All of these estimates should be considered to be very approximate, however, for reasons enumerated elsewhere (Chu et al., 1994a).

The fraction of reaction centers estimated to lack photooxidizable Mn ions in the His-332 mutants is much less than might be expected on the basis of the significant fractions that appear to exhibit charge recombination between Q_A^-

and Y_Z^{ox} after a single flash (Figure 2A−F). This is particularly true for H332E and H332K cells: essentially no PSII reaction centers in H332E cells and only 12−18% of PSII reaction centers in H332K cells appear to lack photooxidizable Mn ions (Figure 3B). Nevertheless, approximately 94% of reaction centers in H332E cells and approximately 90% of reaction centers in H332K cells appear to exhibit charge recombination between Q_A^- and Y_Z^{ox} after a single flash. To explain the apparent discrepancy between the two assays, we propose that electron transfer from Mn to Y_Z^{ox} is unusually slow in the His-332 mutants. We noted previously that charge recombination between Q_A^- and Y_Z^{ox} was unusually rapid in many His-332 mutants, including H332E and H332K (see above). The combination of unusually slow Mn → Y_Z^{ox} and unusually rapid Q_A^- → Y_Z^{ox} electron-transfer reactions could allow Q_A^- to compete successfully with Mn for the reduction of Y_Z^{ox} after a single flash. In such mutants, the reduction of Y_Z^{ox} by Mn would require multiple turnovers (*e.g.*, continuous illumination), as appears to be the case for H332E and H332K cells (Figure 2D,J and 2E,K, respectively). Substantially slowed electron transfer from Mn to Y_Z^{ox} would also explain the substantial progressive quenching observed in H332E and H332K cells (Figure 1D,E) and in other His-332 mutants, such as H332D (Figure 1C).

(iv) Flash-Induced Increases in Fluorescence Yield. In all of the His-332 mutants, the increase in fluorescence yield produced by a saturating flash (relative to F_{max}, see Figure 2A−F) was lower than that in wild-type* cells [the ratio $(F - F_{eq})/(F_{max} - F_{eq})$ was approximately 0.96 in wild-type* cells (Chu et al., 1994a, 1995)]. To determine whether slowed electron transfer from Y_Z to P_{680}^+ contributed to the lower flash-induced increases, we measured the increase produced by the first in a series of saturating flashes given in the presence of DCMU and hydroxylamine (Metz et al., 1989; Chu et al., 1994a, 1995). In all of the His-332 mutants except H332Y, the ratio $(F_1 - F_0)/(F_{max} - F_0)$ was similar to that in wild-type* cells. [The values were 0.51 ± 0.03 for H332Q cells, 0.60 ± 0.06 for H332N cells, 0.58 ± 0.02 for H332D cells, 0.75 ± 0.02 for H332E cells, 0.60 ± 0.05 for H332K cells propagated in dim light, 0.60 ± 0.02 for H332R cells propagated in dim light, 0.65 ± 0.05 for H332S cells propagated in dim light, 0.65 ± 0.02 for H332L cells propagated in dim light, and 0.40 ± 0.08 for H332Y cells propagated in dim light, compared to 0.59 ± 0.06 for wild-type* cells (Chu et al., 1994a).] When the light-sensitive mutants were propagated in normal light, the $(F_1 - F_0)/(F_{max} - F_0)$ ratios decreased to 0.49 ± 0.03, 0.49 ± 0.02, and 0.44 ± 0.08 for H332K, H332R, and H332L cells, respectively, but were essentially unchanged in H332S and H332Y cells. These data imply that slowed electron transfer from Y_Z to P_{680}^+ *may* contribute to the lower flash-induced increases in fluorescence yield observed in the *absence* of hydroxylamine only in H332Y cells when the mutants are propagated in dim light and only in H332K, H332R, H332L and H332Y cells when the mutants are propagated in normal light. In most of the His-332 mutants (Figure 2A−F), the lower flash-induced increases may be caused by the higher equilibrium concentrations of P_{680}^+ present in those reaction centers that lack photooxidizable Mn ions (Chu et al., 1994a, 1995). However, the substantially lower flash-induced increases in H332R cells (Figure 2E) and H332Y cells (not shown), particularly in comparison with H332N cells (Figure 2B), suggest that the lower increases in H332R and H332Y cells may be caused, in part, by the presence of a fluorescence quencher other than P_{680}^+. The presence of such a quencher has been inferred previously in the mutants Δ*psb*O (Philbrick et al., 1991; Chu et al., 1994a), D170R (Chu et al., 1994a), D61A, E65Q, E65A, E189Q, and E189D (Chu et al., 1995).

(v) Requirement for Ca^{2+} Ions. The Ca^{2+} requirements of H332Q, H332N, H332D, H332E, and H332L cells were investigated. When propagated photoheterotrophically in medium containing Na^+ substituted for Ca^{2+}, none of these mutants evolved oxygen and all five exhibited only small increases in fluorescence yield when subjected to saturating flashes in the presence of DCMU and hydroxylamine (not shown). In this respect, H332Q, H332N, H332D, H332E, and H332L cells resembled D59N and D61A cells (Chu et al., 1995): electron transfer from Y_Z to P_{680}^+ appeared to slow dramatically when the cells were propagated in the absence of Ca^{2+} ions. Slowed electron transfer from Y_Z to P_{680}^+ has been observed previously in PSII preparations from a cyanobacterium (Satoh & Katoh, 1985) and from spinach (Boussac et al., 1992) after rigorous depletion of Ca^{2+} ions.

(C) Light Sensitivity and Photoinhibition. The lower apparent PSII contents and slower charge recombination kinetics of H332K, H332R, H332S, H332L, and H332Y cells propagated in normal light *versus* dim light show that these mutants are extremely light-sensitive. This extreme light sensitivity suggests that these mutants are highly susceptible to donor side photoinhibition [for reviews of photoinhibition in PSII, see Prášil et al. (1992) and Aro et al. (1993)]. This type of photoinhibition is believed to involve the accumulation of highly oxidizing radicals on the donor side of PSII [*e.g.*, see Eckert et al. (1991) and Blubaugh et al. (1991)]. We expect that mutants *without* photooxidizable Mn ions (*e.g.*, the mutants D170A, D170N, and D170T) would be significantly *more* light-sensitive than mutants *with* photooxidizable Mn ions because, when illuminated, the equilibrium concentrations of P_{680}^+ and Y_Z^{ox} would be substantially higher in the former. However, as noted previously (Chu et al., 1995), D170A, D170N, and D170T cells are *not* particularly light-sensitive: the apparent PSII contents of these cells are essentially the same as that of wild-type* cells when propagated in normal light, and their fluorescence properties are essentially the same whether propagated in normal or dim light (not shown).

One explanation for the extreme light sensitivity of the H332K, H332R, H332S, H332L, and H332Y mutants is that, when oxidized, the altered or partly assembled Mn clusters in these mutants give off toxic, activated oxygen species, such as hydrogen peroxide. Hydrogen peroxide and superoxide anions can be released when Mn-containing PSII preparations are illuminated and can promote the degradation of PSII polypeptides (Miyao, 1994). Numerous authors have argued that suitably perturbed Mn clusters in PSII release hydrogen peroxide when illuminated [*e.g.*, see Wydrzynski et al. (1989), Bradley et al. (1991), Ananyev et al. (1992), Fine and Frasch (1992), Klimov et al. (1993), and Hillier and Wydrzynski (1993)]. In addition, several authors have suggested that Cl^- ions prevent the binding of water or hydroxide ions to the Mn cluster in the lower S states to prevent the premature oxidation of a water-derived ligand in the S_2 or S_3 state (Rutherford, 1989; Thompson et al., 1989; Fine & Frasch, 1992). The premature oxidation of a water-derived ligand in the perturbed Mn clusters of H332K,

H332R, H332S, H332L, and H332Y cells could explain the extreme light sensitivity of these mutants. This mechanism of photoinhibition has been postulated previously (Bradley et al., 1991; Jegerschöld et al., 1992). Chloride-depleted PSII membranes from spinach are highly sensitive to photoinduced damage (Jegerschöld et al., 1990; Jegerschöld & Styring, 1991). The initial step of photoinhibition, determined to be the loss of 1−2 Mn ions from PSII, has been postulated to result from the formation of hydrogen peroxide by the altered Mn cluster (Jegerschöld et al., 1992). The Mn cluster is also the initial site of photoinduced damage in a mutant of *Chlamydomonas reinhardtii* that lacks the extrinsic 23 kDa polypeptide and that, therefore, has an elevated requirement for Cl^- ions (Rova et al., 1994).

In Cl^--depleted PSII membranes, DCMU protects against photoinduced damage (Jegerschöld et al., 1990). This protection suggests that the postulated formation of hydrogen peroxide may require the formation of the altered S_3 state. In the light-sensitive His-332 mutants, those reaction centers that contain photooxidizable Mn ions photoaccumulated Q_A^- relatively slowly during continuous illumination (Figure 3B). Because the premature oxidation of a water-derived ligand by the Mn cluster in a perturbed S_2 state would trap Q_A^- by generating the $S_1Q_A^-$ state (or possibly $S_0Q_A^-$), the slow rates of Q_A^- photoaccumulation in the light-sensitive His-332 mutants suggest that the postulated formation of hydrogen peroxide in these mutants requires a Mn oxidation state higher than can be generated in the presence of DCMU (*e.g.*, a state higher than S_2 if the Mn clusters in these mutants resemble wild-type clusters in terms of structure and oxidation states).

(D) Involvement in Mn Binding. All of the His-332 mutants except H332D and H332E contain substantial fractions of PSII reaction centers that lack photooxidizable Mn ions (Figure 3A,B). These results show that His-332 influences the assembly and/or stability of the Mn cluster. However, because all mutants contain a substantial fraction of reaction centers that *contain* photooxidizable Mn ions, His-332 probably does not ligate the first Mn^{2+} ion that binds during the assembly of the Mn cluster. Nevertheless, it may ligate a Mn ion that subsequently binds. Nixon, Diner, and co-workers arrived at similar conclusions. In preliminary accounts, these authors reported that the high-affinity Mn^{2+} binding site first occupied is unperturbed in His-332 mutants (Diner et al., 1991; Nixon et al., 1992; Nixon & Diner, 1994; Tang et al., 1994b).

In proteins, histidine ligates metal ions predominantly with its $\epsilon 2$ (or τ) nitrogen (Chakrabarti, 1990b). The $\delta 1$ (or π) nitrogen of such residues typically forms a hydrogen bond with a peptide carbonyl group or with a carboxylate residue (Chakrabarti, 1990b). This hydrogen bond helps orient the His residue. In addition, the strength of this hydrogen bond modulates the strength of the His−metal interaction (Christianson & Alexander, 1989; Chakrabarti, 1990b; Goodin & McRee, 1993). Both Gln and Glu functionally replace the $\epsilon 2$ nitrogen of His as a ligand to Fe in the structure of cytochrome *c* peroxidase (Sundaramoorthy et al., 1992; Choudhury et al., 1992, 1994). On the basis of chemical considerations, Glu, Asp, Gln, Asn, His, Ser, Thr, and Tyr are all considered to be potential ligands of Mn in PSII (Pecoraro, 1988; Brudvig & Crabtree, 1989; Wieghardt, 1989). Therefore, our observations of significant oxygen evolution activity in H332Q and H332S cells (Table 1) and of photooxidizable Mn in 95−100% of reaction centers in H332D and H332E cells (Figure 3A,B) are consistent with the ligation of Mn by His-332, probably with its $\epsilon 2$ nitrogen. If this hypothesis is correct, then the smaller size and relative inflexibility of Asn could explain the lack of oxygen evolution activity and the relative lack of photooxidizable Mn ions in H332N cells (Figure 3A). Ligation of the Mn cluster by the smaller, inflexible Ser and Asp residues would require structural changes for accommodation. However, the small size of Ser may permit the ligation of Mn by an immobilized water molecule or by another species. Exogenous substances can replace His-117 as a ligand to Cu in the H117G mutant of azurin (den Blaauwen & Canters, 1993) and His-93 as a ligand to Fe in the H93G mutant of sperm whale myoglobin (Barrick, 1994; DePillis et al., 1994).

The normal S-state cycle has been postulated to involve the possible formation of an imidazolate bridge between Mn ions (Tang et al., 1994a) and the oxidation of a histidine residue in the S_3 state [*e.g.*, see Boussac et al. (1990)]. However, if Gln replaces His-332 as a ligand to Mn, the significant oxygen evolution activity observed in H332Q cells (Table 1) implies that the histidine residue(s) potentially oxidized or recruited as a bridging ligand does not include His-332 (at least not under normal, physiological conditions). In ribulose-1,5-bisphosphate carboxylase/oxygenase, the binding of substrate is postulated to displace His as ligand of the active-site Mg^{2+} ion (Haining & McFadden, 1994). Because the replacement of this residue with Glu eliminates catalytic activity, it has been postulated that substrate cannot displace Glu from Mg^{2+} in this mutant because of the stronger Glu−Mg^{2+} interaction (Haining & McFadden, 1994). If the structural changes that normally accompany the $S_3 \rightarrow (S_4) \rightarrow S_0$ transition in PSII involve the displacement of His-332 from the Mn cluster, a similar inability to displace Asp or Glu may partly explain the absence of oxygen evolution activity in H332D and H332E cells.

The charge recombination kinetics of H332D cells after a single flash (Figure 2C) or 5 s of illumination (Figure 2I) resembles that of wild-type* cells more than any other His-332 mutant. If simple electrostatic interactions govern the S_2/S_1 midpoint potential, then the S_2 state should be stabilized in H332D cells if Asp replaces His-332 as a ligand to Mn. That this state appears to be *destabilized* in most His-332 reaction centers in H332D cells (Figure 2C) suggests either that the factors that govern the S_2/S_1 midpoint potential are more complex, that the Mn clusters in H332D cells differ considerably from those in wild-type* cells, or that Asp does not ligate Mn.

If Gln replaces His-332 as a ligand to Mn, then one might expect Glu to substitute as well [*e.g.*, see Choudhury et al. (1994)]. Indeed, the slower $Q_A^- \rightarrow$ Mn charge recombination kinetics observed after 5 s of illumination in H332E cells (Figure 2J) suggests that the S_2 state is stabilized in this mutant, as would be expected from simple electrostatic considerations (see above). However, the fluorescence properties of H332E and H332K cells are similar (Figures 1 and 2). Furthermore, the fluorescence properties of H332R and H332L cells do not differ dramatically from those of H332K cells. Although Lys replaces Met as a ligand to Fe in cytochrome *c* from yeast (Ferrer et al., 1993) and in cytochrome *c*-550 from *Thiobacillus versutus* (Ubbink et al., 1994), and Arg replaces Met (Hampsey et al., 1986) and possibly His (Sorrell et al., 1989; Garcia et al., 1992) as a

ligand to Fe in cytochrome *c* from yeast, Leu is an unlikely ligand for a metal ion. Therefore, the similarity of the fluorescence properties of H332E, H332K, H332R, and H332L cells suggests that, if His-332 ligates Mn, then neither Glu, Lys, or Arg replaces it as a ligand. Possibly the charge of Glu prevents it from occupying the same positions as His or Gln. In cytochrome *bo* ubiquinol oxidase from *Escherichia coli*, Asn can replace His-419 as an apparent ligand to heme, but Asp cannot (Calhoun et al., 1993). In H332E cells, Glu may cause structural perturbations that permit the missing histidyl nitrogen to be replaced by either another residue, a peptide carbonyl oxygen, or a water molecule. Alternatively, the Mn clusters in these cells may differ considerably from those in wild-type* cells. Possibly the charge and/or bulk of Lys, Arg, Leu, and Tyr cause perturbations similar to those caused by Glu. However, the Mn clusters in H332E cells must differ substantially from those in H332K, H332R, H332L, and H332Y cells: unlike H332K, H332R, H332L, and H332Y cells, H332E cells are *not* extremely light-sensitive. The differences between the Mn clusters in H332E cells and the light-sensitive Mn clusters in other mutants may become apparent only in Mn oxidation states higher than can be obtained in the presence of DCMU (*e.g.*, in altered S_3 states). Significant structural changes have been proposed to accompany the $S_2 \rightarrow S_3$ transition in normal PSII particles [for reviews, see Debus (1992), Rutherford et al. (1992), and Renger (1993)]. Perhaps analogous structural changes in H332K, H332R, H332L, and H332Y cells lead to the premature oxidation of a water-derived ligand.

The preceding discussion has emphasized the possibility that His-332 ligates the Mn cluster. However, an alternate possibility is that His-332 serves as a crucial hydrogen bond donor in PSII and that its influence on the assembly and/or stability of the Mn cluster is indirect. In sperm whale myoglobin, His-64 provides a crucial hydrogen bond to O_2 (and to an immobilized water molecule in deoxymyoglobin). This hydrogen bond is retained in the H64Q and H64G mutants (the latter via an immobilized water molecule), but not in the H64L mutant (Quillin et al., 1993). In ribulose-1,5-bisphosphate carboxylase/oxygenase, a His residue that interacts with substrate can be replaced with Gln (but not with Ala, Lys, or Arg) with some retention of catalytic activity (Haining & McFadden, 1994). A determination of whether or not His-332 ligates the Mn cluster in PSII will require spectroscopic analysis of mutant PSII particles. For example, if His-332 contributes one of the imidazole nitrogens detected in recent ESEEM studies (Tang et al., 1994a), the detected signal should diminish or disappear in PSII particles isolated from H332D or H332E cells. Of all of the His-332 mutants examined, these mutants may be the most amenable to spectroscopic studies of isolated PSII particles because nearly all of the PSII reaction centers in these mutants appear to contain photooxidizable Mn ions *in vivo* (Figure 3A,B).

(E) Involvement in Ca^{2+} Binding. As noted earlier, electron transfer from Y_Z to P_{680}^+ appeared to slow dramatically when H332Q, H332N, H332D, H332E, or H332L cells were propagated in the absence of Ca^{2+} ions. These results imply that the affinity of PSII for Ca^{2+} in these mutants is too low to utilize the quantities of adventitious Ca^{2+} present in our Ca^{2+}-depleted growth medium, quantities that *are* sufficient to sustain the normal growth of wild-type* cells and many mutants (Chu et al., 1995). It is unlikely that His would directly coordinate a Ca^{2+} ion in PSII [*e.g.*, see McPhalen et al. (1991)]. Therefore, the diminished affinity of mutant His-332 reaction centers for Ca^{2+} must be caused by mutation-induced structural perturbations. However, because the binding of Ca^{2+} to PSII is believed to occur *after* assembly of the Mn cluster (Tamura & Cheniae, 1988; Miller & Brudvig, 1989; Tamura et al., 1989), the diminished affinity for Ca^{2+} in the His-332 mutants may be caused by the perturbations in the Mn clusters in these mutants.

(II) Glu-333

(A) Growth, Oxygen Evolution Characteristics, and PSII Contents of Mutants. The following mutants were constructed: E333Q, E333D, E333N, E333H, E333A, and E333Y. All mutants except E333Q required glucose for propagation, even in dim light (Table 2). In normal light, E333Q cells could be propagated in the absence of glucose, but only on solid medium. However, when propagated in dim light, E333Q cells grew photoautotrophically at essentially the same rate as wild-type* cells (the A_{730} doubling times were 105−120 h for wild-type* cells and 105−145 h for E333Q cells, data not shown). Only E333Q cells evolved oxygen at significant rates compared to wild-type* cells (36% ± 9% when propagated in dim light, 19% ± 5% when propagated in normal light; see Table 2). This oxygen-evolving activity was lost rapidly in saturating light. The apparent PSII contents of all the Glu-333 mutants were depressed compared to wild-type* cells (Table 2). The apparent PSII contents of E333D, E333A, and E333Y cells diminished significantly when propagated in normal light (Table 2). Surprisingly, the apparent PSII content of E333Q cells appeared to be slightly *higher* when propagated in *normal* light.

(B) Fluorescence Characteristics of Mutants. (i) Electron Transfer to Y_Z^{ox}. The fluorescence yields that followed each of four saturating flashes spaced 50 ms apart are shown in Figure 4 for the mutants E333Q, E333D, E333H, and E333Y (all cells were propagated in dim light). When propagated in dim light, the data of the E333N and E333A mutants (not shown) resembled those of E333Y cells. In all of the Glu-333 mutants, the maximum fluorescence yield after the second and subsequent flashes was partly quenched. The most extensive quenching was observed in E333D and E333H cells (Figure 4B,C). Indeed, the progressive quenching observed in the E333H mutant resembled that in mutants that lack photooxidizable Mn ions [*e.g.*, the mutants D170A, D170N, and D170T (Chu et al., 1994a)]. In all of the Glu-333 mutants, the extent of quenching diminished as the spacing between the saturating flashes was increased, becoming negligible at flash spacings of 600−800 ms (not shown). These data show that the reduction of Y_Z^{ox} is slowed dramatically in all of the Glu-333 mutants: a considerable fraction of Y_Z^{ox} remains oxidized for at least 50 ms following each saturating flash (Chu et al., 1994a).

In all of the Glu-333 mutants, significant amounts of Q_A^- remained reduced 50 ms after each flash (Figure 4). These amounts decreased as the spacing between the saturating flashes was increased (not shown), showing that the slowest components of electron transfer from Q_A^- to Q_B were slowed significantly in these mutants, especially in E333D and E333H cells. Similar slowing of this electron-transfer step

Table 2: Comparison of Glu-333 Mutant Strains

strain	growth light intensity (μE m^{-2} s^{-1})	photoautotrophic growth[a]	O_2 evolution[b] (% of wt*)	apparent PSII content[c] (% of wt*)	kinetics of Q_A^- oxidation after a single flash[d] (%)	k^{-1} (s)	no. of cultures included in analyses
E333Q	5–6	+	36 ± 9	65 ± 10	37 ± 5	0.05 ± 0.01	4
					32 ± 5	0.42 ± 0.04	
					31 ± 3	3.4 ± 0.5	
	50–60	+ (slow[e])	19 ± 5	90 ± 17	44 ± 4	0.05 ± 0.03	6
					28 ± 4	0.42 ± 0.14	
					28 ± 4	4.4 ± 1.1	
E333D	5–6	–	0	58 ± 12	57 ± 2	0.021 ± 0.003	3
					26 ± 2	0.31 ± 0.03	
					17 ± 1	3.4 ± 0.5	
	50–60	–	0	41 ± 5	44 ± 5	0.07 ± 0.03	5
					28 ± 2	0.77 ± 0.12	
					28 ± 5	7.6 ± 0.7	
E333N	5–6	–	0	41 ± 6	48 ± 20	0.055 ± 0.020	2
					35 ± 18	0.26 ± 0.17	
					16 ± 2	4.9 ± 1.2	
	50–60	–	0	48 ± 3	45 ± 13	0.09 ± 0.04	4
					23 ± 5	0.87 ± 0.03	
					32 ± 8	10 ± 3	
E333H	5–6	–	0	58 ± 12	52 ± 8	0.05 ± 0.02	3
					30 ± 9	0.24 ± 0.05	
					18 ± 2	5.5 ± 1.1	
	50–60	–	0	62 ± 12	56 ± 6	0.13± 0.04	2
					19 ± 1	0.83 ± 0.08	
					26 ± 5	8.6 ± 1.3	
E333A	5–6	–	0	43 ± 2	50 ± 8	0.05 ± 0.02	2
					32 ± 6	0.35 ± 0.10	
					18 ± 3	9.5 ± 1.7	
	50–60	–	0	22 ± 7	42 ± 8	0.05 ± 0.02	4
					28 ± 11	0.64 ± 0.29	
					30 ± 13	6.2 ± 1.6	
E333Y	5–6	–	0	59 ± 1	39 ± 3	0.13 ± 0.01	3
					22 ± 3	0.97 ± 0.12	
					40 ± 1	9.2 ± 0.8	
	50–60	–	0	54 ± 8	32 ± 6	0.08 ± 0.05	4
					25 ± 5	0.73 ± 0.35	
					44 ± 2	8.7 ± 1.4	

[a] Measured in growth medium without glucose. [b] Initial rates measured in growth medium. The eight wild-type* cultures used in this study evolved 680 ± 30 μmol of O_2 (mg of Chl)$^{-1}$ h^{-1} (Chu et al., 1994a). [c] Estimated from the total yield of variable chlorophyll *a* fluorescence ($F_{max} - F_0$). For E333D and E333Q cells propagated at 50–60 μE m^{-2} s^{-1}, these estimates have been shown to correlate with those estimated from [^{14}C]DCMU binding studies (Chu et al., 1994a). For the other mutants and growth conditions listed, this correlation is assumed. [d] Measured in the presence of DCMU and analyzed by assuming three exponentially decaying components. The relative amplitude (%) and the inverse of the rate constant of each component are reported. See left panels of Figure 5. [e] On solid medium only.

was noted previously in other mutants, including most of the His-332 mutants (see above).

(ii) Charge Recombination between Q_A^- and PSII Electron Donors. The decay of fluorescence yield that followed a saturating flash given to E333Q, E333D, E333H, and E333Y cells in the presence of DCMU is shown in Figure 5A–D (all cells were propagated in dim light). When propagated in dim light, the E333N and E333A mutants (not shown) exhibited data similar to those of E333H cells, except that the maximum flash-induced increase in fluorescence yield in E333A cells was lower (see the following) and the slowest decay component decayed more slowly. The amplitudes and rates of the decay kinetics in all six mutants (propagated in both dim and normal light) are presented in Table 2. All six mutants exhibited significant amounts of rapid decay kinetics that presumably correspond to charge recombination between Q_A^- and Y_Z^{ox}. The lowest amounts of rapid decay were exhibited by E333Q and E333Y cells (Figure 5A,D), while the highest amount was exhibited by E333D cells (Figure 5B). In E333Q, E333D, E333N, and E333H cells (Table 2), the rates of the slower decay components were similar to those in wild-type* cells (Table 1), although the slowest decay component was slightly slower in E333N and E333H cells. In all four of these mutants, the two slower components presumably correspond to charge recombination between Q_A^- and an oxidized form of a multinuclear Mn cluster. If we assume that charge recombination between Q_A^- and P_{680}^+ is not altered by the mutations, the rates of the decay components suggest that the S_2/S_1 midpoint potential in E333Q cells is similar to that in wild-type* cells, while the oxidized forms of the Mn clusters in E333N and E333H cells are somewhat stabilized with respect to the S_2 state in wild-type* cells. The slowest decaying components in E333A and E333Y cells exhibited inverse rate constants of 9.4–9.5 s, which are similar to the rates of the slowest components in H332R, H332L, and H332Y cells (see above) and in mutants that lack the extrinsic 33 kDa polypeptide (Chu et al., 1994b). As discussed in relation to the His-332 mutants, this slow decay could correspond to charge recombination between Q_A^- and either a single oxidized Mn^{3+} ion or a Mn cluster of unknown nuclearity (Chu et al., 1994b).

The charge recombination kinetics of E333D, E333N, E333H, and E333A cells slowed considerably when these mutants were propagated in normal light instead of in dim light (Table 2). These results show that E333D, E333N, E333H, and E333A cells are extremely light-sensitive. The

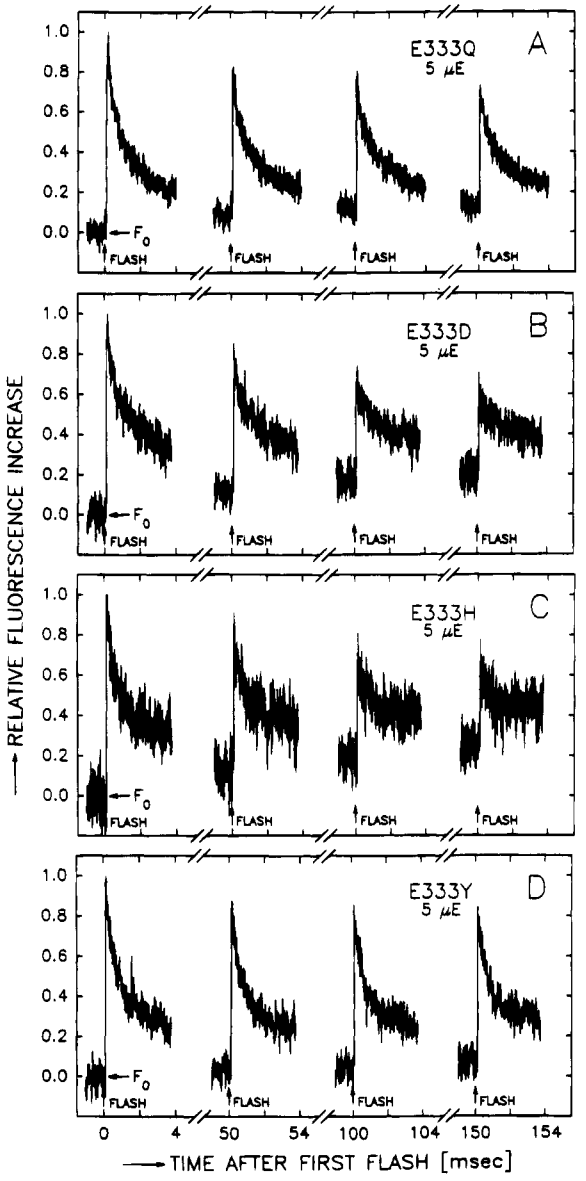

FIGURE 4: Yield of variable chlorophyll *a* fluorescence produced by each of four saturating flashes given at 50 ms intervals to Glu-333 mutant cells. Five milliseconds of data are shown for each flash. (A) E333Q; (B) E333D; (C) E333H; (D) E333Y. The conditions were the same as in Figure 1. The maximum $(F - F_0)/F_0$ values measured after the first flash in each series were 0.24 for (A), 0.12 for (B), 0.08 for (C), and 0.11 for (D). The data of E333N and E333A cells (not shown) resembled those of E333Y cells, except that the maximum $(F - F_0)/F_0$ values were 0.09 and 0.08, respectively. All cells were propagated in dim light. Six individual flash series were averaged for (A) and (B) each, five for (C), and 7 for (D). The frequency of the monitoring flashes was switched from 1.6 to 100 kHz for 5 ms beginning 1 ms before each flash.

E333Q cells are also light-sensitive, as shown by the higher oxygen-evolving rate of these cells when propagated in dim light (Table 2). However, E333Q cells exhibited no appreciable change in their fluorescence properties when propagated in normal instead of dim light (*e.g.*, Table 2). Interestingly, the charge recombination kinetics of E333Y cells (Figure 5D) resembled those of mutants that lack the extrinsic 33 kDa polypeptide even when propagated in dim light.

(iii) Photoaccumulation of Q_A^-. To estimate the fractions of PSII reaction centers in the Glu-333 mutants that contain photooxidizable Mn ions, cells were illuminated for 1−15 s

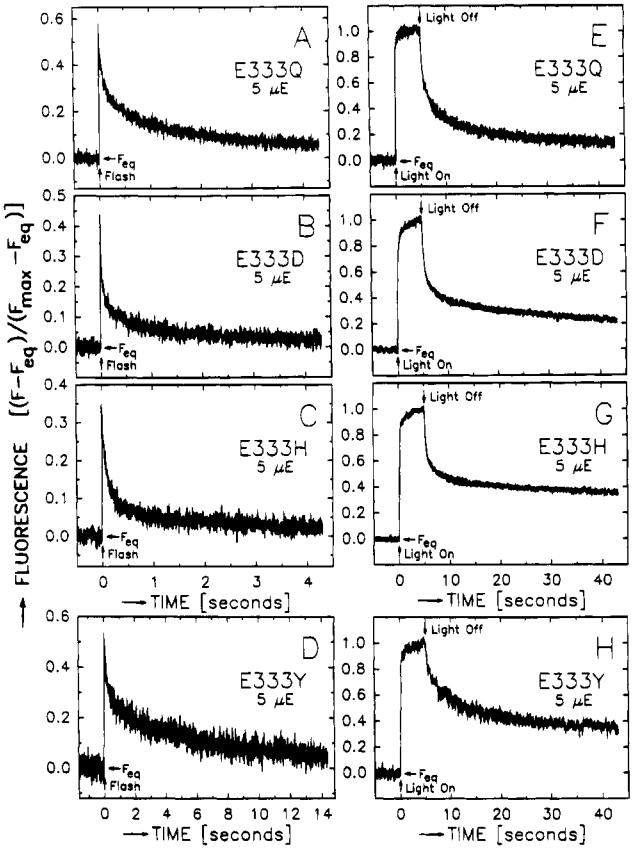

FIGURE 5: Formation and decay of Q_A^- in response to a saturating flash (left panels) or to 5 s of illumination (right panels) given to Glu-333 mutant cells in the presence of DCMU, as measured by changes in the yield of chlorophyll *a* fluorescence: (A, E) E333Q; (B, F) E333D; (C, G) E333H; (D, H) E333Y. The data of E333N and E333A cells (not shown) resembled those of E333H cells. All cells were propagated in dim light. Note the three different time scales employed in this figure. The conditions were the same as in Figure 2. Traces A−D represent the computer averages of 16−18 traces. The monitoring flashes were applied at 1.6 kHz.

in the presence of DCMU. The kinetics of Q_A^- oxidation in E333Q, E333D, E333H, and E333Y cells after 5 s of illumination are presented in Figure 5E−H. All cells were propagated in dim light. The data of E333N and E333A cells (propagated in dim light, not shown) resembled those of E333H cells. As with most other mutants (Chu et al., 1994a), the rates of the two *faster* components of Q_A^- oxidation after 5 s of illumination (Figure 5E−H) were roughly similar to the rates of the two *slower* components observed after a single flash (Figure 5A−D, Table 2). The E333D mutant resembled the His-332 mutants in that the amplitudes of these components were smaller after a single flash than after 5 s of illumination. As discussed in relation to the His-332 mutants, both of these components presumably correspond to charge recombination between Q_A^- and an oxidized form of a Mn cluster (Chu et al., 1994a). The fractions of Q_A^- that *photoaccumulated* during 5 s of illumination were 23% ± 4% in E333Q cells (Figure 5E), 37% ± 5% in E333D cells (Figure 5F), 41% ± 2% in E333N cells (not shown), 40% ± 6% in E333H cells (Figure 5G), 48% ± 3% in E333A cells (not shown), and 43% ± 2% in E333Y cells (Figure 5H), compared to 7.2% ± 0.9% in wild-type* cells (Chu et al., 1994a). Figure 6A shows the fraction of Q_A^- that photoaccumulated during 1−15 s of illumination in E333Q, E333D, and E333N cells (propagated in dim light) in comparison to wild-type* and D170A cells. Figure 6B

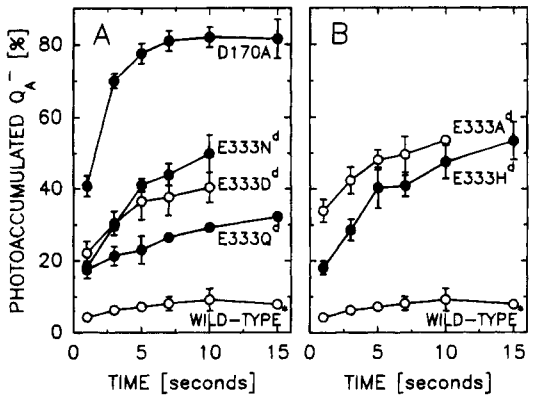

FIGURE 6: Fraction of PSII reaction centers in Glu-333 mutant cells that photoaccumulated Q_A^- after illumination for specific intervals of time (see Figure 5E–H and text): (A) photoaccumulation of Q_A^- in E333Q, E333D, and E333N cells in comparison to wild-type* and D170A cells; (B) photoaccumulation of Q_A^- in E333H and E333A cells in comparison to wild-type* cells. The data of E333Y cells (not shown) resembled those of E333A cells. All cells were propagated in dim light. The wild-type* and D170A data are taken from Chu et al. (1994a) to facilitate comparisons. The conditions were the same as in Figure 3.

shows the corresponding data for E333H and E333A cells (propagated in dim light). The data of E333Y cells propagated in dim light (not shown) overlapped those of E333A cells.

In all mutants, the rates of Q_A^- photoaccumulation were heterogeneous, with a fraction of PSII reaction centers photoaccumulating Q_A^- during the first second of illumination, and other fractions photoaccumulating at slower rates. In E333N and E333H cells (and possibly in E333D, E333A, and E333Y cells), the slower components of Q_A^- photoaccumulation were considerably more rapid than in wild-type* cells. In most PSII mutants previously examined, the rate of photoaccumulation correlated with the equilibrium concentration of P_{680}^+ (Chu et al., 1994a). For example, in Mn-containing PSII reaction centers, rapid Q_A^- photoaccumulation correlated with rapid $Q_A^- \rightarrow S_2$ charge recombination kinetics. In contrast, the kinetics of $Q_A^- \rightarrow$ Mn charge recombination was unusually rapid in *none* of the Glu-333 mutants. Therefore, factors other than electron donation from cytochrome *b*-559 and/or Y_D to P_{680}^+ (Chu et al., 1994a) must contribute to the photoaccumulation of Q_A^- in E333N and E333H cells, and possibly in E333D, E333A, and E333Y cells as well. This point will be discussed further in the following.

The data of Figure 6A,B imply that a considerable fraction of PSII reaction centers in all of the Glu-333 mutants lack photooxidizable Mn ions *in vivo*. By comparing the extent of Q_A^- photoaccumulation after 7–10 s of illumination with that in wild-type* and D170A cells, we estimate that up to 24–28% of E333Q reaction centers, 39–43% of E333D reaction centers, 48–56% of E333N reaction centers, 44–56% of E333H reaction centers, 53–61% of E333A reaction centers, and 57–60% of E333Y reaction centers lack photooxidizable Mn ions *in vivo*. These estimates should be considered to be very approximate for reasons enumerated elsewhere (Chu et al., 1994a). Furthermore, in E333N and E333H cells (and possibly in E333D, E333A, and E333Y cells as well), these estimates are probably upper limits because, as noted in the preceding paragraph, additional factors must contribute to the photoaccumulation of Q_A^- in these mutants compared to other mutants. Indeed, in E333Y cells, only 39% ± 3% of Q_A^- appears to recombine with Y_Z^{ox} after a single saturating flash given in the presence of DCMU (Figure 5D, Table 2), suggesting that more reaction centers in E333Y cells contain photooxidizable Mn ions than was estimated on the basis of the Q_A^- photoaccumulation data. Nevertheless, in all other mutants except E333D, the estimated fraction of reaction centers that lack photooxidizable Mn ions is in rough agreement with the fraction of Q_A^- that appears to recombine with Y_Z^{ox} after a single saturating flash given in the presence of DCMU (Figure 5A–F). In E333D cells, charge recombination between Q_A^- and Y_Z^{ox} was unusually rapid (Figure 5B, Table 2). Consequently, Q_A^- may compete successfully with Mn for the reduction of Y_Z^{ox} in a significant fraction of reaction centers in this mutant.

(iv) Flash-Induced Increases in Fluorescence Yield. In all of the Glu-333 mutants, the increase in fluorescence yield produced by a saturating flash (relative to F_{max}, see Figure 5A–D) was lower than in wild-type* cells [the ratio $(F - F_{eq})/(F_{max} - F_{eq})$ was approximately 0.96 in wild-type* cells (Chu et al., 1994a, 1995)]. The lower flash-induced increase was particularly evident in E333H (Figure 5C), E333N (not shown), and E333A cells (not shown). [The maximum $(F - F_{eq})/(F_{max} - F_{eq})$ values were approximately 0.38 and 0.26 in E333N and E333A cells, respectively.] To determine whether slowed electron transfer from Y_Z to P_{680}^+ contributed to any of the lower flash-induced increases, we measured the increase produced by the first in a series of saturating flashes given in the presence of DCMU and hydroxylamine (Metz et al., 1989; Chu et al., 1994a, 1995). In all of the Glu-333 mutants except E333H and E333A, the ratio $(F_1 - F_0)/(F_{max} - F_0)$ was similar to that in wild-type* cells. [The values were 0.54 ± 0.03 for E333Q cells, 0.56 ± 0.07 for E333D cells, 0.52 ± 0.11 for E333N cells, 0.49 ± 0.07 for E333H cells, 0.44 ± 0.07 for E333A, and 0.53 ± 0.06 for E333Y cells (all cells were propagated in dim light), compared to 0.59 ± 0.06 for wild-type* cells (Chu et al., 1994a).] When propagated in normal light, the $(F - F_{eq})/(F_{max} - F_{eq})$ ratios decreased to 0.26 ± 0.04 in E333A cells and to approximately 40% in E333Y cells. These data imply that slowed electron transfer from Y_Z to P_{680}^+ *may* contribute to the lower flash-induced increases in fluorescence yield observed in the *absence* of hydroxylamine only in E333H and E333A cells when the mutants are propagated in dim light and only in E333H, E333A, and E333Y cells when the mutants are propagated in normal light. In most of the Glu-333 mutants (Figure 5A–D), the lower flash-induced increases may be caused by the higher equilibrium concentrations of P_{680}^+ present in those reaction centers that lack photooxidizable Mn ions (Chu et al., 1994a, 1995). However, the lower flash-induced increases in E333H, E333N, and E333A cells, particularly in comparison with E333D cells (Figure 5B), suggest that the lower increases in E333H, E333N, and E333A cells may be caused, in part, by the presence of a fluorescence quencher other than P_{680}^+. The presence of such a quencher has been inferred previously in several mutants, including H332R and H332Y (see above).

(v) Requirement for Ca^{2+} Ions. The Ca^{2+} requirements of E333Q and E333D cells were investigated. When propagated photoheterotrophically in medium containing Na^+ substituted for Ca^{2+}, neither mutant evolved oxygen, and both exhibited only small increases in fluorescence yield when

subjected to saturating flashes in the presence of DCMU and hydroxylamine (not shown). In this respect, E333Q and E333D cells resembled the His-332 mutants (see above) and D59N and D61A cells (Chu et al., 1995): electron transfer from Y_Z to P_{680}^+ appeared to slow dramatically when the cells were propagated in the absence of Ca^{2+} ions.

(C) Light Sensitivity and Photoinhibition. The lower oxygen-evolving activity of E333Q cells, the lower apparent PSII contents of E333D and E333A cells, and the slower charge recombination kinetics of E333D, E333N, E333H, and E333A cells propagated in normal rather than dim light show that these five mutants are extremely light-sensitive. In this respect, all of the Glu-333 mutants except E333Y resembled the light-sensitive His-332 mutants H332K, H332R, H332S, H332L, and H332Y. Because a similar light sensitivity is not observed in mutants that lack photooxidizable Mn ions, we have proposed that the altered or partly assembled Mn clusters in the light-sensitive His-332 mutants prematurely oxidize a water-derived ligand and give off toxic, activated oxygen species, such as hydrogen peroxide (see above). We propose that a similar mechanism operates in the Glu-333 mutants. However, because the slow components of Q_A^- photoaccumulation are unusually rapid in some of the Glu-333 mutants, we suggest that the premature oxidation of a water-derived ligand in E333H and E333N cells (and possibly in E333D, E333A, and E333Y cells) may occur in a Mn oxidation state than can be readily generated in the presence of DCMU (*e.g.*, in an altered S_2 state). In contrast, higher Mn oxidation states may be required in the light-sensitive His-332 mutants (see above). As noted earlier, numerous authors have argued that suitably perturbed Mn clusters in PSII release hydrogen peroxide when illuminated, and several authors have suggested that Cl^- ions prevent the premature oxidation of a water-derived ligand in the S_2 or S_3 state.

(D) Involvement in Mn Binding. All of the Glu-333 mutants contain substantial fractions of PSII reaction centers that lack photooxidizable Mn ions (Figure 6A,B). These results show that Glu-333 influences the assembly and/or stability of the Mn cluster. However, because all mutants contain a substantial fraction of reaction centers that *contain* photooxidizable Mn ions, Glu-333, like His-332, probably does not ligate the first Mn^{2+} ion that binds during assembly of the Mn cluster. Indeed, in a preliminary account, Nixon and Diner reported that the high-affinity Mn^{2+} binding site first occupied is unperturbed in Glu-333 mutants (Nixon & Diner, 1994). Because E333Q cells evolve oxygen at significant rates, and because Gln can serve as a ligand to Fe in cytochrome *c* peroxidase (Sundaramoorthy et al., 1992; Choudhury et al., 1992, 1994), one possibility is that Glu-333 ligates a Mn ion that binds subsequent to the first. If so, the smaller size and relative inflexibility of Asp and Asn may prevent these residues from substituting for Glu-333 as effectively as Gln. Similarly, His and Tyr may fail to substitute for steric reasons. However, if Glu-333 ligates Mn, the apparent similarity of the S_2/S_1 midpoint potentials in E333Q and wild-type* cells would imply that Glu-333 exerts little or no influence on the redox properties of the Mn cluster.

(E) Involvement in Ca^{2+} Binding. An alternate possibility is that Glu-333 ligates a Ca^{2+} ion. The apparent slowing of electron transfer from Y_Z to P_{680}^+ when E333Q and E333D cells were propagated photoheterotrophically in the absence of Ca^{2+} ions demonstrates that the affinity of PSII for Ca^{2+} in these mutants is too low to utilize the quantities of adventitious Ca^{2+} present in our Ca^{2+}-depleted growth media. If Glu-333 ligates a Ca^{2+} ion in PSII, then the diminished affinity of E333Q reaction centers for Ca^{2+} ions would be expected [*e.g.*, see Maune et al. (1992) and Babu et al. (1992)]. However, if Glu-333 ligates Ca^{2+}, it is difficult to explain why mutations such as E333Q would alter the stability and/or assembly of the Mn cluster: the binding of Ca^{2+} to PSII is believed to occur *after* assembly of the Mn cluster (Tamura & Cheniae, 1988; Miller & Brudvig, 1989; Tamura et al., 1989). Furthermore, the D59N and D61A mutations decrease the affinity of PSII for Ca^{2+} ions *without* disturbing the assembly and/or stability of the Mn cluster (Chu et al., 1995). It seems more likely that Glu-333 does not ligate Ca^{2+} in PSII. As in the His-332 mutants described earlier, the diminished affinity for Ca^{2+} ions in the Glu-333 mutants may be caused by the perturbations in the Mn clusters in these mutants.

(F) A Possible Structural Role. Although we cannot exclude the possibility that Glu-333 ligates Mn in PSII, the differences in the oxygen-evolving and fluorescence characteristics of E333Q and E333D cells suggest that, like Glu-189 (Chu et al., 1995), Glu-333 may perform a crucial structural role in optimizing water oxidation. Possibly Glu-333 participates in a network of hydrogen bonds that can be partly maintained by Gln, but not by the shorter and less flexible Asp and Asn residues and not by His, Ala, or Tyr. In dihydrofolate reductase, the hydrogen bond network involving Asp-27 is maintained in the D27N mutation: an O−HN hydrogen bond is merely replaced by an NH−N hydrogen bond (Howell et al., 1986). The substitution of Glu by Asp is not always a conservative mutation [*e.g.*, see Richardson and Richardson (1989)]. Indeed, there are several examples where a Glu → Asp substitution is deleterious to function because the position and orientation of the carboxylate moiety have changed in the structure of the mutant protein [*e.g.*, the E43D mutation in staphylococcal nuclease (Loll & Lattman, 1990) and the E165D mutation in triosephosphate isomerase (Joseph-McCarthy et al., 1994)]. Furthermore, there are examples where the Asp → Glu mutation is far more deleterious than the Asp → Asn mutation [*e.g.*, see Babu et al. (1992) and Mizrahi et al. (1994)]. In PSII, one possibility is that the proposed network of hydrogen bonds involving Glu-333 is crucial for positioning a residue that ligates a Mn ion. The improper positioning of this residue in the Glu-333 mutants could decrease the stability of the Mn cluster or the probability of its correct assembly.

(III) His-337

(A) Growth, Oxygen Evolution Characteristics, and PSII Contents of Mutants. The following mutants were constructed: H337R, H337Q, H337N, H337E, H337D, H337Y, H337V, and H337L. In addition, the H337F mutant was obtained as a spontaneous pseudorevertant of H337V cells. Only the H337R, H337F, H337Q, and H337N mutants could be propagated in the absence of glucose. In normal light, H337R cells grew at the same rate as wild-type* cells, whereas H337F cells grew at a slower rate (the A_{730} doubling times were approximately 15 and 50 h for H337R and H337F cells, respectively). In normal light, the H337Q and H337N cells could be propagated photoautotrophically only on solid

Table 3: Comparison of His-337 Mutant Strains

strain	growth light intensity (μE m^{-2} s^{-1})	photoautotrophic growth[a]	O_2 evolution[b] (% of wt*)	apparent PSII content[c] (% of wt*)	kinetics of Q_A^- oxidation after a single flash[d] (%)	k^{-1} (s)	no. of cultures included in analyses
H337R	50−60	+	51 ± 2	84 ± 9	29 ± 11	0.05 ± 0.03	3
					55 ± 9	0.27 ± 0.05	
					16 ± 2	4.8 ± 0.7	
H337Q	5−6	+ (slow)	36 ± 4	69 ± 6	25 ± 2	0.05 ± 0.01	5
					52 ± 4	0.68 ± 0.06	
					23 ± 8	4.6 ± 0.2	
	50−60	+ (slow[e])	31 ± 8	62 ± 9	24 ± 2	0.06 ± 0.03	5
					52 ± 4	0.71 ± 0.15	
					24 ± 5	5.0 ± 1.4	
H337N	50−60	+ (slow[e])	18 ± 4	53 ± 13	26 ± 4	0.045 ± 0.020	6
					40 ± 4	0.67 ± 0.08	
					34 ± 4	6.5 ± 1.6	
H337E	5−6	−	17 ± 1	74 ± 12	27 ± 5	0.05 ± 0.03	4
					42 ± 4	0.73 ± 0.22	
					31 ± 6	4.3 ± 0.9	
	50−60	−	0	43 ± 4	36 ± 6	0.19 ± 0.07	3
					29 ± 11	1.7 ± 0.6	
					35 ± 10	9.9 ± 3.2	
H337D	5−6	−	5 ± 2	61 ± 15	38 ± 10	0.16 ± 0.07	3
					27 ± 8	1.5 ± 0.9	
					35 ± 3	11 ± 4	
	50−60	−	0	43 ± 7	32 ± 8	0.11 ± 0.06	4
					28 ± 5	0.89 ± 0.27	
					41 ± 5	7.0 ± 2.6	
H337Y	5−6	−	0−3	42 ± 11	27 ± 5	0.09 ± 0.03	3
					19 ± 3	1.1 ± 0.2	
					53 ± 8	8.8 ± 1.1	
	50−60	−	0	5 ± 2	nd[f]	nd[f]	3
H337V	50−60	−	0	38 ± 7	29 ± 5	0.08 ± 0.06	5
					27 ± 7	1.0 ± 0.4	
					44 ± 2	8.5 ± 0.6	
H337L	50−60	−	12 ± 5	62 ± 8	75 ± 2	0.0041 ± 0.0004	3
					13 ± 2	0.31 ± 0.09	
					13 ± 3	2.9 ± 0.8	
H337F	50−60	+(slow)	37 ± 1	102 ± 16	54 ± 1	0.0042 ± 0.0001	3
					10 ± 1	0.36 ± 0.06	
					36 ± 2	2.8 ± 0.3	

[a] Measured in growth medium without glucose. [b] Initial rates measured in growth medium. The eight wild-type* cultures used in this study evolved 680 ± 30 μmol of O_2 (mg of Chl)$^{-1}$ h^{-1} (Chu et al., 1994a). [c] Estimated from the total yield of variable chlorophyll *a* fluorescence ($F_{max} - F_0$). For H337Q and H337L cells propagated at 50−60 μE m^{-2} s^{-1}, these estimates have been shown to correlate with those estimated from [^{14}C]DCMU binding studies (Chu et al., 1994a). For the other mutants and growth conditions listed, this correlation is assumed. [d] Measured in the presence of DCMU and analyzed by assuming three exponentially decaying components. The relative amplitude (%) and the inverse of the rate constant of each component are reported. See left panels of Figure 8. [e] On solid medium only. [f] Not done.

medium. In dim light, H337Q cells (but not H337N cells) could also be grown photoautotrophically in liquid medium, although growth was slow (the A_{730} doubling time was approximately 170 h, compared to 105−120 h for wild-type* cells grown under these conditions). Several mutants evolved oxygen at significant rates compared to wild-type* cells (Table 3). The highest rates were exhibited by H337R and H337F cells (51% ± 2% and 37% ± 1%, respectively). The oxygen-evolving activities of H337E and H337D cells were higher when propagated in dim light (Table 3). In H337E, H337N, H337L, and H337D cells, the oxygen-evolving activity was rapidly lost in saturating light.

The apparent PSII contents of all of the His-337 mutants except H337F were somewhat depressed compared to wild-type* cells (Table 3). The apparent PSII contents of H337E, H337D, and H337Y cells were considerably higher when propagated in dim light (Table 3). In contrast, the apparent PSII contents (and light-saturated oxygen evolution rates) of H337R, H337F, and H337L cells were *lower* when propagated in dim light, while those of H337N and H337V cells were essentially unchanged. The H337L mutant was sensitive to *darkness*: when incubated in darkness, H337L cells lost essentially all of their oxygen-evolving activity in 30 min. In this respect, H337L cells resemble Δ*psb*O cells, which also rapidly lose oxygen-evolving activity in darkness (Chu et al., 1994b; R. L. Burnap, personal communication).

(B) Fluorescence Characteristics of Mutants. (i) Electron Transfer to Y_Z^{ox}. The fluorescence yields that followed each of four saturating flashes spaced 50 ms apart are shown in Figure 7 for the mutants H337R, H337Q, H337L, H337F, H337E, and H337D (the H337E and H337D cells were propagated in dim light). The data of H337N and H337V cells (not shown) resembled those of H337Q cells. When propagated in dim light, the data of H337Y cells (not shown) resembled those of H337F and H337D cells. Little or no quenching of the maximal yield after any flash was observed in H337R, H337L, and H337E cells (Figure 7A,C,E, respectively). In contrast, the maximum fluorescence yield after the second and subsequent flashes was partly quenched in H337Q, H337F, and H337D cells (Figure 7B,D,F, respectively) and in H337N and H337V cells (not shown). The most extensive quenching was observed in H337Q, H337N, and H337V cells. However, even the amount of quenching observed in these cells was relatively moderate

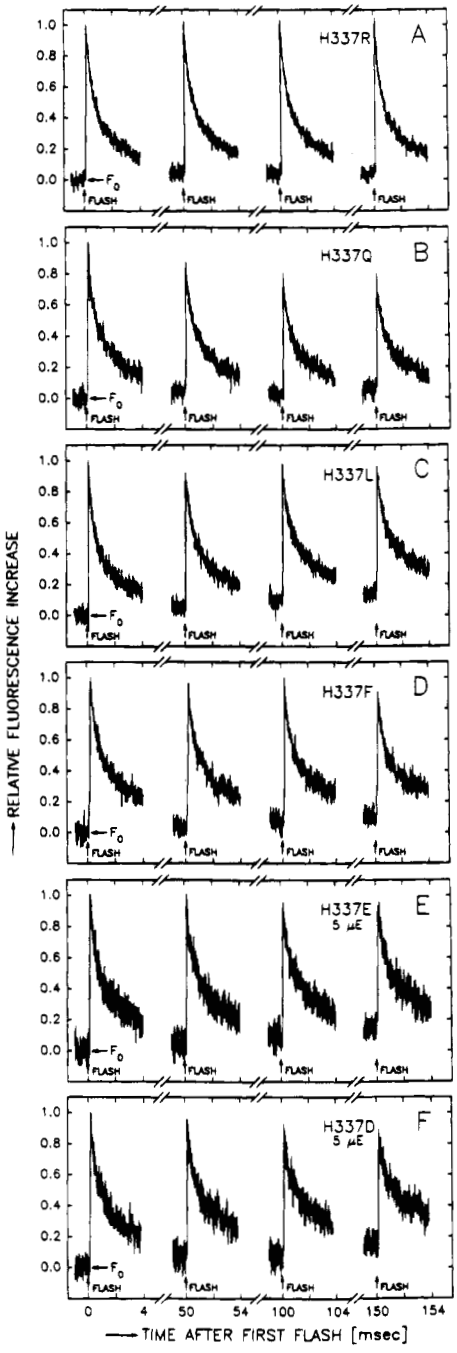

FIGURE 7: Yield of variable chlorophyll *a* fluorescence produced by each of four saturating flashes given at 50 ms intervals to His-337 mutant cells. Five milliseconds of data are shown for each flash. (A) H337R; (B) H337Q; (C) H337L; (D) H337F; (E) H337E; (F) H337D. The H337E and H337D cells were propagated in dim light. The conditions were the same as in Figure 1. The maximum $(F - F_0)/F_0$ values measured after the first flash in each series were 0.30 for (A), 0.24 for (B), 0.22 for (C), 0.30 for (D), 0.17 for (E), and 0.11 for (F). Four individual flash series were averaged for (A), (B), (C), and (D) each, and six for (E) and (F) each. The data of H337N and H337V cells (not shown) resembled those of H337Q cells, except that the maximum $(F - F_0)/F_0$ values were 0.23 and 0.06, respectively. The data of H337Y cells (not shown, propagated in dim light) resembled those of H337F and H337D cells, except that the maximum $(F - F_0)/F_0$ ratio was 0.06. The frequency of the monitoring flashes was switched from 1.6 to 100 kHz for 5 ms beginning 1 ms before each flash.

in comparison to that observed in various Glu-189, His-332, and Glu-333 mutants [see above and see Chu et al. (1995)]. In all of the His-337 mutants that exhibited progressive quenching, the extent of quenching diminished as the spacing between the saturating flashes was increased, becoming negligible at flash spacings of 200−400 ms (not shown). These data show that the reduction of Y_Z^{ox} is slowed dramatically in only some of the His-337 mutants.

In each mutant except H337R, significant amounts of Q_A^- remained reduced 50 ms after each flash (Figure 7). These amounts decreased as the spacing between the saturating flashes was increased (not shown), showing that the slowest components of electron transfer from Q_A^- to Q_B were slowed significantly in these mutants, especially in H337L, H337F, H337E, H337D, and H337Y cells. Similar slowing of this electron-transfer step was noted previously in other mutants, including most of those at His-332 and all of those at Glu-333 (see above).

(ii) Charge Recombination between Q_A^- and PSII Electron Donors. The decay of fluorescence yield that followed a saturating flash given to H337R, H337Q, H337L, H337F, H337E, and H337D cells in the presence of DCMU is shown in Figure 8A−F (the H337E and H337D cells were propagated in dim light). The data of H337N cells (not shown) resembled those of H337Q cells, while the data of H337Y cells propagated in dim light (not shown) and H337V cells (not shown) resembled those of H337D cells. The amplitudes and rates of the decay kinetics in all nine mutants are presented in Table 3. In most of the mutants, 25−30% of the decay kinetics was rapid, presumably corresponding to charge recombination between Q_A^- and Y_Z^{ox}. The highest amounts of rapid decay were exhibited by H337F and H337L cells (54% ± 1% and 75% ± 2%, respectively, see Figure 8C,D). In these two mutants, the apparent rate of charge recombination between Q_A^- and Y_Z^{ox} was unusually rapid, exhibiting inverse rate constants of 4.1−4.2 ms (Table 3). By assuming that charge recombination between Q_A^- and P_{680}^+ was not altered by the mutations, these results imply that the Y_Z^{ox}/Y_Z midpoint potential increased significantly in the H337F and H337L mutants, as previously concluded for H332N, H332D, H332E, and H332K cells (see above) and for D170A and D170S cells (Chu et al., 1994a, 1995).

In H337F and H337L cells, the rates of the slower decay components (Table 3) were similar to those of wild-type* cells (Table 1). These rates were slightly slower in H337Q, H337N, and H337E cells (the H337E cells were propagated in dim light). In contrast, in H337R cells, one of the two slower components decayed more rapidly, and the other more slowly, than in wild-type* cells. Similar behavior was noted earlier for the H332D mutant. Because all of these His-337 mutants evolved oxygen at significant rates, the two slower components presumably correspond to charge recombination between Q_A^- and altered S_2 states. By assuming that charge recombination between Q_A^- and P_{680}^+ was not altered by the mutations, the rates of the slower decay components suggest that the S_2/S_1 midpoint potential in H337F and H337L cells is similar to that in wild-type* cells, is slightly lower in H337Q, H337N, and H337E cells, and is slightly *higher* in many reaction centers in H337R cells. The slowest decaying components in H337D, H337Y, and H337V cells exhibited inverse rate constants of 8.5−11 s, which are similar to the rates of the slowest components in mutants that lack the extrinsic 33 kDa polypeptide (Chu et al., 1994b) and in a number of His-332 and Glu-333 mutants (see above). As discussed in relation to the His-332 and Glu-333 mutants, this slow decay could correspond to charge recombination

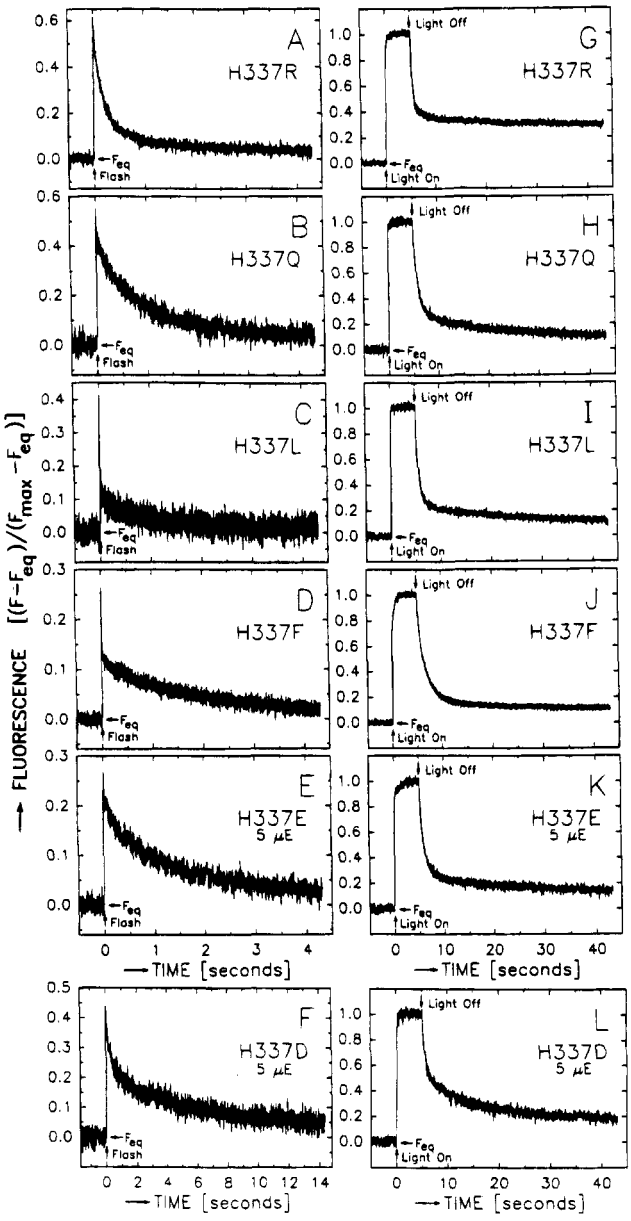

FIGURE 8: Formation and decay of Q_A^- in response to a saturating flash (left panels) or to 5 s of illumination (right panels) given to His-337 mutant cells in the presence of DCMU as measured by changes in the yield of chlorophyll *a* fluorescence: (A, G) H337R; (B, H) H337Q; (C, I) H337L; (D, J) H337F; (E, K) H337E; (F, L) H337D. The H337E and H337D cells were propagated in dim light. The data of H337N cells (not shown) resembled those of H337Q cells, while the data of H337V cells (not shown) and H337Y cells (not shown, propagated in dim light) resembled those of H337D cells. Note the three different time scales employed in this figure. The conditions were the same as in Figure 2. Traces A−F represent the computer averages of 12, 6, 8, 15, 16, and 16 traces, respectively. The monitoring flashes were applied at 1.6 kHz.

between Q_A^- and either a single oxidized Mn^{3+} ion or a Mn cluster of unknown nuclearity (Chu et al., 1994b).

The charge recombination kinetics of H337E cells slowed considerably when propagated in normal light instead of in dim light (Table 3). These results show that the H337E mutant is extremely light-sensitive. Interestingly, the charge recombination kinetics of H337D, H337V, and H337Y cells resembled those of mutants that lack the extrinsic 33 kDa polypeptide even when propagated in dim light (*e.g.*, see Figure 8F). In contrast, the charge recombination kinetics of the dark-sensitive H337L mutant slowed considerably in

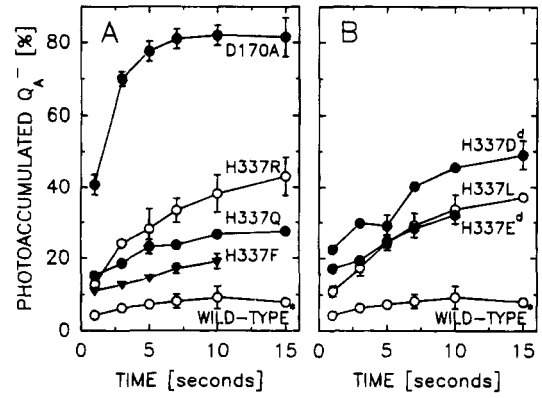

FIGURE 9: Fraction of PSII reaction centers in His-337 mutant cells that photoaccumulated Q_A^- after illumination for specific intervals of time (see Figure 8G−L and text): (A) photoaccumulation of Q_A^- in H337F, H337Q, and H337R cells in comparison to wild-type* and D170A cells; (B) photoaccumulation of Q_A^- in H337E, H337L, and H337D cells in comparison to wild-type* cells. The H337E and H337D cells were propagated in dim light. The data of H337N cells (not shown) resembled those of H337E cells. The wild-type* and D170A data are taken from Chu et al. (1994c) to facilitate comparisons. The conditions were the same as in Figure 3.

darkness, gradually changing from mostly very rapid to mostly very slow kinetics (similar to those of mutants that lack the extrinsic 33 kDa polypeptide) over 3−5 h of incubation in darkness.

(iii) Photoaccumulation of Q_A^-. To estimate the fractions of PSII reaction centers in the His-337 mutants that contain photooxidizable Mn ions, cells were illuminated for 1−15 s in the presence of DCMU. The kinetics of Q_A^- oxidation in H337R, H337Q, H337L, H337F, H337E, and H337D cells after 5 s of illumination are presented in Figure 8G−L. The H337E and H337D cells were propagated in dim light. The data of H337N cells (not shown) resembled those of H337Q cells, while the data of H337V and H337Y cells (the latter propagated in dim light) resembled those of H337D cells. In all of the His-337 mutants, the rates of the two *faster* components of Q_A^- oxidation after 5 s of illumination (Figure 8G−L) were roughly similar to the rates of the two *slower* components observed after a single flash (Figure 8A−F, Table 3). The H337L and H337F mutants resembled the His-332 mutants in that the amplitudes of these components were smaller after a single flash than after 5 s of illumination. As discussed previously, both of these components presumably correspond to charge recombination between Q_A^- and an oxidized form of a Mn cluster (Chu et al., 1994a). The fractions of Q_A^- that *photoaccumulated* during 5 s of illumination were 30% ± 5% in H337R cells (Figure 8G), 23% ± 2% in H337Q cells (Figure 8H), 23% ± 2% in H337N cells (not shown), 25% ± 2% in H337E cells propagated in dim light (Figure 8K), 29% ± 3% in H337D cells propagated in dim light (Figure 8L), 31% ± 4% in H337Y cells propagated in dim light (not shown), 27% ± 3% in H337V cells (not shown), 24% ± 3% in H337L cells (Figure 8I), and 15% ± 1% in H337F cells (Figure 8L), compared to 7.2% ± 0.9% in wild-type* cells (Chu et al., 1994a). Figure 9A shows the fraction of Q_A^- that photoaccumulated during 1−15 s of illumination in H337R, H337Q, and H337F cells, in comparison to that in wild-type* and D170A cells. Figure 9B shows the corresponding data for H337D, H337L, and H337E cells (the H337D and H337E cells were propagated in dim light). The data for H337N cells (not shown) overlapped those of H337E cells, while

those of H337V and H337Y cells (the latter propagated in dim light) were 23−29% and 30−31%, respectively, at 3, 5, and 7 s of illumination (not shown).

In all mutants, the rates of Q_A^- photoaccumulation were heterogeneous, with a fraction of PSII reaction centers photoaccumulating Q_A^- during the first second of illumination, and other fractions photoaccumulating at slower rates. In H337R, H337E, H337D, H337N, and H337L cells, the slower components of Q_A^- photoaccumulation were considerably more rapid than that in wild-type* cells. In H337R cells, the more rapid photoaccumulation rate correlated with the more rapid $Q_A^- \rightarrow S_2$ charge recombination kinetics observed in this mutant, as observed previously in other mutants (Chu et al., 1994a). In contrast, the kinetics of $Q_A^- \rightarrow$ Mn charge recombination was unusually rapid in none of the other His-337 mutants. Therefore, factors other than electron donation from cytochrome *b*-559 and/or Y_D to P_{680}^+ (Chu et al., 1994a) must contribute to the photoaccumulation of Q_A^- in H337E, H337D, H337N, and H337L cells. The rapid photoaccumulation in H337E and H337D cells may be related to the extreme light sensitivity of these mutants, whereas the rapid photoaccumulation in H337L cells may be related to this mutant's dark sensitivity (see the following).

The data of Figure 9A,B imply that a considerable fraction of PSII reaction centers in all of the His-337 mutants lack photooxidizable Mn ions *in vivo*. By comparing the extent of Q_A^- photoaccumulation after 5−10 s of illumination with that in wild-type* and D170A cells, we estimate that 10−14% of H337F reaction centers, 21−24% of H337Q reaction centers, 22−26% of H337V reaction centers, 23−28% of H337N reaction centers, 24−34% of H337L reaction centers, 25−30% of H337E reaction centers, 31−34% of H337Y reaction centers, 32−40% of H337R reaction centers, and 37−50% of H337D reaction centers lack photooxidizable Mn ions *in vivo*. These estimates should be considered to be very approximate for reasons enumerated elsewhere (Chu et al., 1994a). Furthermore, in all mutants except H337Q, H337F, H337V, and H337Y, these estimates are probably upper limits because, as noted in the preceding paragraph, additional factors must contribute to the photoaccumulation of Q_A^- in these mutants compared to other cells. Nevertheless, in all mutants except H337L and H337F, the estimated fraction of reactions center that lack photooxidizable Mn ions is in rough agreement with the fraction of Q_A^- that appears to recombine with Y_Z^{ox} after a single saturating flash given in the presence of DCMU (Figure 8A−F). In H337L and H337F cells, the unusually rapid charge recombination between Q_A^- and Y_Z^{ox} (Figure 8C,D, Table 3) suggests that Q_A^- may compete successfully with Mn for the reduction of Y_Z^{ox} in a significant fraction of reaction centers in these mutants.

(iv) Flash-Induced Increases in Fluorescence Yield. In all of the His-337 mutants, the increase in fluorescence yield produced by a saturating flash (relative to F_{max}, see Figure 8A−F) was lower than that in wild-type* cells [the ratio $(F - F_{eq})/(F_{max} - F_{eq})$ was approximately 0.96 in wild-type* cells (Chu et al., 1994a, 1995)]. The lower flash-induced increase was particularly evident in H337F and H337E cells (Figure 8D,E). [The maximum $(F - F_{eq})/(F_{max} - F_{eq})$ values were approximately 0.44, 0.46, and 0.46 in H337N, H337V, and H337Y cells, respectively.] To determine whether slowed electron transfer from Y_Z to P_{680}^+ contributed to any of the lower flash-induced increases, we measured the increase produced by the first in a series of saturating flashes given in the presence of DCMU and hydroxylamine (Metz et al., 1989; Chu et al., 1994a, 1995). In all of the His-337 mutants except H337Y, the ratio $(F_1 - F_0)/(F_{max} - F_0)$ was similar to that in wild-type* cells. [The values were 0.67 ± 0.08 for H337R cells, 0.66 ± 0.02 for H337Q cells, 0.62 ± 0.03 for H337N cells, 0.52 ± 0.09 for H337E cells propagated in dim light, 0.67 ± 0.06 for H337D cells propagated in dim light, 0.48 ± 0.07 for H337Y cells propagated in dim light, 0.59 ± 0.06 for H337V cells, and 0.64 ± 0.02 for H337L cells, compared to 0.59 ± 0.06 for wild-type* cells (Chu et al., 1994a).] The values for H337E and H337D cells did not decrease significantly when these cells were propagated in normal light. These data imply that slowed electron transfer from Y_Z to P_{680}^+ *may* contribute to the lower flash-induced increases in fluorescence yield observed in the *absence* of hydroxylamine only in H337Y cells. In some of the His-337 mutants (*e.g.*, in H337R and H337Q), the lower flash-induced increases may be caused by the higher equilibrium concentrations of P_{680}^+ present in those reaction centers that lack photooxidizable Mn ions (Chu et al., 1994a, 1995). However, the lower flash-induced increases in H337F and H337E cells, particularly in comparison with H337L and H337D cells, respectively, suggest that the lower increases in H337F and H337E cells (and possibly in other His-337 mutants as well) may be caused, in part, by the presence of a fluorescence quencher other than P_{680}^+. The presence of such a quencher has been inferred previously in several His-332, Glu-333, and other mutants (see above).

(v) Requirement for Ca^{2+} Ions. The Ca^{2+} requirements of H337Q and H337N cells were investigated. When propagated photoheterotrophically in medium containing Na^+ substituted for Ca^{2+}, neither mutant evolved oxygen and both exhibited only small increases in fluorescence yield when subjected to saturating flashes in the presence of DCMU and hydroxylamine (not shown). In this respect, H337Q and H337N cells resembled the His-332 and Glu-333 mutants and D59N and D61A cells: electron transfer from Y_Z to P_{680}^+ appeared to be slowed dramatically when the cells were propagated in the absence of Ca^{2+} ions.

(C) Light Sensitivity and Photoinhibition. The lower oxygen-evolving activity of H337E cells, the lower apparent PSII contents of H337E, H337D, and H337Y cells, and the slower charge recombination kinetics of H337E cells propagated in normal light instead of in dim light show that these mutants are extremely light-sensitive. In this respect, these His-337 mutants resembled the Glu-333 mutants and the five light-sensitive His-332 mutants. Because similar light sensitivity is not observed in mutants that lack photooxidizable Mn ions, we have proposed that the altered or partly assembled Mn clusters in the light-sensitive His-332 and Glu-333 mutants prematurely oxidize a water-derived ligand and give off toxic, activated oxygen species, such as hydrogen peroxide (see above). We propose that a similar mechanism operates in H337E, H337D, and H337Y cells. Furthermore, the rapid photoaccumulation of Q_A^- in H337E and H337D cells suggests that the premature oxidation may occur in the altered S_2 states of these mutants, as proposed for the E333H and E333N mutants (see above).

The slower components of Q_A^- photoaccumulation were also unusually rapid in H337L cells (Figure 9B). This mutant does not appear to be unusually light-sensitive. However,

it rapidly loses oxygen-evolving activity in darkness, presumably because of reduction of the Mn cluster. Perhaps the species responsible for this reduction is an even more effective donor when the Mn cluster is oxidized to the S_2 state.

(D) Involvement in Mn Binding. All of the His-337 mutants contain substantial fractions of PSII reaction centers that lack photooxidizable Mn ions (Figure 9A,B). These results show that His-337 influences the assembly and/or stability of the Mn cluster. However, because most of the PSII reaction centers in all of the His-337 mutants *contain* photooxidizable Mn ions, His-337, like His-332 and Glu-333, probably does not ligate the first Mn^{2+} ion that binds during assembly of the Mn cluster. To evaluate the possibility that His-337 ligates a Mn^{2+} ion that binds subsequently, we first discuss the mutants H337V, H337L, and H337F. Because of their chemical nature, neither Val, Leu, nor Phe would be expected to ligate a metal ion. Indeed, the lack of oxygen evolution, the low apparent PSII content, and the slow charge recombination kinetics of the H337V mutant (Table 3), even when propagated in dim light, show that the H337V mutation severely disrupts the assembly or operation of the Mn cluster. Therefore, it is curious that Leu and Phe, being progressively larger and bulkier than Val, are progressively less disruptive than Val when substituted for His-337: both the H337L and H337F mutants evolved oxygen at significant rates (Table 3). Indeed, H337F cells were weakly photoautotrophic and contained essentially the same apparent PSII content as wild-type* cells (Table 3). To explain this peculiarity and the sharply disparate properties of the H337F and H337Y mutants (*e.g.*, see Table 3), we propose that the hydrophobicity and bulk of Leu and Phe cause structural perturbations that permit the missing His-337 imidazole moiety to be replaced by another residue, a peptide carbonyl oxygen, or a water molecule. We previously invoked such compensatory, mutation-induced structural rearrangements to explain the significant oxygen-evolving activities of D170V, D170L, and D170I cells (Chu et al., 1995). There are ample precedents for compensatory, mutation-induced structural rearrangements in other systems [*e.g.*, in ferredoxin I of *Azotobacter vinelandii* (Martín et al., 1990), ricin A (Kim et al., 1992), and human alcohol dehydrogenase (Stone et al., 1993)]. That the H337L and H337F mutations cause structural changes is evident from the unusually rapid $Q_A^- \rightarrow Y_Z^{ox}$ charge recombination kinetics observed in these mutants (Figure 8C,D, Table 3). These unusually rapid kinetics imply the existence of mutation-induced alterations in the Y_Z^{ox}/Y_Z midpoint potential. We previously invoked mutation-induced structural changes to explain the unusually rapid $Q_A^- \rightarrow Y_Z^{ox}$ charge recombination kinetics observed in D170S and D170A cells (Chu et al., 1995). On the basis of the preceding considerations, we conclude that the oxygen-evolving and growth characteristics of H337L and H337F cells do not eliminate His-337 as a possible ligand of the Mn cluster in PSII.

Because Arg apparently can replace His as a ligand to Fe in cytochrome *c* (Sorrell et al., 1989; Garcia et al., 1992), because and Gln can replace His as a ligand to Fe in cytochrome *c* peroxidase (Sundaramoorthy et al., 1992; Choudhury et al., 1992, 1994), the photoautotrophic growth and oxygen evolution rates of H337R and H337Q cells suggest that His-337 may ligate the Mn cluster, probably with its $\epsilon 2$ (or τ) nitrogen (Chakrabarti, 1990b). Seibert and co-workers have long argued that His-337 ligates the Mn cluster on the basis of chemical modification and proteolysis studies (Preston & Seibert, 1990, 1991b).

If His-337 ligates the Mn cluster, the smaller size and relative inflexibility of Asn and Asp may prevent these residues from substituting for His-337 as effectively as Gln. Similarly, Tyr may fail to substitute for steric reasons. If Arg and Gln replace His-337 as a ligand to Mn, the oxygen-evolving activity of H337R and H337Q cells implies that the histidine residue(s) potentially oxidized [*e.g.*, see Boussac et al. (1990)] or potentially recruited as a bridging ligand (Tang et al., 1994a) during the S-state cycle does not include His-337 (at least not under normal physiological conditions). However, if His-337 ligates Mn, it is curious that Glu is a relatively ineffective substitute, especially because Glu can replace His as a ligand to Fe in cytochrome *c* peroxidase (Choudhury et al., 1994) and because the apparent S_2/S_1 midpoint potentials of the H337Q and H337E mutants are similar (Figure 8B,E, Table 3). Perhaps the lower *initial* light-saturated oxygen evolution rate of the H337E mutant reflects this mutant's extreme light sensitivity. However, the similarity of the apparent S_2/S_1 midpoint potentials in the H337E and H337Q mutants is particularly curious given the apparent destabilization of the S_2 state in H337R cells: the apparent destabilization of the S_2 state in H337R cells suggests that, if His-337 ligates Mn, this residue influences the redox properties of the Mn cluster.

An alternate possibility is that His-337 serves as a crucial hydrogen bond donor and that its influence on the assembly and/or stability of the Mn cluster is indirect. Both Arg and Gln are good hydrogen bond donors that can potentially substitute for His. As noted earlier, in sperm whale myoglobin, His-64 provides a crucial hydrogen bond to O_2 that is retained in the H64Q and H64G mutants, but not in the H64L mutant (Quillin et al., 1993). The retention of some catalytic activity in ribulose-1,5-bisphosphate carboxylase/oxygenase when Gln replaced a His residue that interacts with substrate (Haining & McFadden, 1994) was also noted. A determination of whether or not His-337 ligates the Mn cluster in PSII will require the spectroscopic analysis of mutant PSII particles as described earlier in relation to the His-332 mutants.

(E) Involvement in Ca^{2+} Binding. As noted earlier, electron transfer from Y_Z to P_{680}^+ appeared to slow dramatically when H337Q or H337N cells were propagated in the absence of Ca^{2+} ions. These results imply that the affinity of PSII for Ca^{2+} in these mutants is too low to utilize the quantities of adventitious Ca^{2+} present in our Ca^{2+}-depleted growth media, quantities that *are* sufficient to sustain the normal growth of wild-type* cells and many mutants (Chu et al., 1995). It is unlikely that His would directly coordinate a Ca^{2+} ion in PSII [*e.g.*, see McPhalen et al. (1991)]. Because the binding of Ca^{2+} to PSII is believed to occur *after* assembly of the Mn cluster (Tamura & Cheniae, 1988; Miller & Brudvig, 1989; Tamura et al., 1989), the diminished affinity for Ca^{2+} in the His-337 mutants may be caused by the perturbations in the Mn clusters in these mutants.

(IV) Asp-342

(A) Growth, Oxygen Evolution Characteristics, and PSII Contents of Mutants. The following mutants were constructed: D342E, D342N, D342H, and D342A. All mutants

Table 4: Comparison of Asp-342 Mutant Strains

strain	growth light intensity (μE m^{-2} s^{-1})	photoautotrophic growth[a]	O_2 evolution[b] (% of wt*)	apparent PSII content[c] (% of wt*)	kinetics of Q_A^- oxidation after a single flash[d] (%)	k^{-1} (s)	no. of cultures included in analyses
D342E	50−60	+ (slow)	20 ± 4	86 ± 14	33 ± 7	0.04 ± 0.02	7
					57 ± 5	0.28 ± 0.06	
					10 ± 2	4.7 ± 1.4	
D342N	5−6	−	33 ± 6	60 ± 7	50 ± 4	0.013 ± 0.003	3
					26 ± 3	0.58 ± 0.11	
					24 ± 5	3.7 ± 0.9	
	50−60	−	3 ± 1	34 ± 10	35 ± 6	0.06 ± 0.03	5
					33 ± 5	1.2 ± 0.5	
					32 ± 9	9.3 ± 2.6	
D342H	5−6	−	6 ± 1	41 ± 9	41 ± 8	0.085 ± 0.030	4
					28 ± 6	1.4 ± 0.3	
					31 ± 11	9.7 ± 1.4	
	50−60	−	0	46 ± 3	26 ± 12	0.09 ± 0.04	4
					25 ± 4	0.86 ± 0.37	
					48 ± 4	8.9 ± 2.7	
D342A	50−60	−	0	31 ± 6	30 ± 11	0.05 ± 0.02	6
					26 ± 5	1.1 ± 0.5	
					45 ± 8	9.2 ± 2.1	

[a] Measured in growth medium without glucose. [b] Initial rates measured in growth medium. The eight wild-type* cultures used in this study evolved 680 ± 30 μmol of O_2 (mg of Chl)$^{-1}$ h^{-1} (Chu et al., 1994a). [c] Estimated from the total yield of variable chlorophyll *a* fluorescence ($F_{max} - F_0$). For D342E, D342N, and D342A cells propagated at 50−60 μE m^{-2} s^{-1}, these estimates have been shown to correlate with those estimated from [^{14}C]DCMU binding studies (Chu et al., 1994a). For the other mutants and growth conditions listed, this correlation is assumed. [d] Measured in the presence of DCMU and analyzed by assuming three exponentially decaying components. The relative amplitude (%) and the inverse of the rate constant of each component are reported. See left panels of Figure 11.

except D342E required glucose for propagation, even in dim light (Table 4). The D342E mutant grew somewhat more slowly than wild-type* cells in the absence of glucose, exhibiting a A_{730} doubling time of 17−21 h compared to 13−18 h for wild-type* cells (data not shown). The D342E mutant did not grow photoautotrophically when Ca^{2+} was omitted from the BG-11 growth medium: neither Sr^{2+}, Mg^{2+}, nor Na^+ would substitute. When propagated in normal light, only D342E cells evolved oxygen at significant rates compared to wild-type* cells (20% ± 4%, see Table 4), although a trace of oxygen evolution was evident in D342N cells (3% ± 1%). However, when the mutants were propagated in dim light, the oxygen-evolving activity of D342N cells increased substantially (to 33% ± 6%), and some activity was observed in D342H cells (6% ± 1%). (The oxygen-evolving activity of D342E and D342A cells did not increase when propagated in dim light.) The oxygen-evolving activity of D342E, D342N, and D342H cells was lost rapidly in saturating light. Like the H337L mutant (see above), D342E cells were sensitive to *darkness*, losing about half of their oxygen-evolving activity during 3 h of incubation in darkness (not shown). In this respect, D342E cells were much less sensitive to darkness than H337L or Δ*psb*O cells [see above and Chu et al. (1994a)].

The apparent PSII contents of all four Asp-342 mutants were depressed compared to wild-type* cells (Table 4). The apparent PSII content of D342N cells decreased substantially when propagated in normal light (Table 4). In contrast, the apparent PSII contents of D342E, D342H, and D342A cells were approximately the same whether propagated in normal or dim light.

(B) Fluorescence Characteristics of Mutants. (i) Electron Transfer to Y_Z^{ox}. The fluorescence yields that followed each of four saturating flashes spaced 50 ms apart are shown in Figure 10 for the mutants D342E, D342N, D342H, and D342A (the D342N and D342H cells were propagated in dim light). In D342E and D342N cells, the maximum fluorescence yield after each flash was essentially the same (Figure 10A,B). However, in D342H and D342A cells, the maximum fluorescence yield after the second and subsequent flashes was partly quenched (Figure 10C,D). In both of these mutants, the extent of quenching diminished as the spacing between the saturating flashes was increased, becoming negligible at flash spacings of 200−400 ms (not shown). These data show that the reduction of Y_Z^{ox} is slowed significantly in only the D342H and D342A mutants, with only small fractions of Y_Z^{ox} remaining oxidized for at least 50 ms following each saturating flash (Chu et al., 1994a).

In each mutant except D342E, significant amounts of Q_A^- remained reduced 50 ms after each flash (Figure 10). These amounts decreased as the spacing between the saturating flashes was increased (not shown), showing that the slowest components of electron transfer from Q_A^- to Q_B were slowed significantly in D342N, D342H, and D342A cells. Similar slowing was noted earlier in most of the His-332, Glu-333, and His-337 mutants (see above).

(ii) Charge Recombination between Q_A^- and PSII Electron Donors. The decay of fluorescence yield that followed a saturating flash given to D342E, D342N, D342H, and D342A cells in the presence of DCMU is shown in Figure 11A−D (the D342N and D342H cells were propagated in dim light). The amplitudes and rates of the decay kinetics are presented in Table 4. All four mutants exhibited significant amounts of rapid decay kinetics that presumably corresponds to charge recombination between Q_A^- and Y_Z^{ox}. The lowest amounts of rapid decay were exhibited by D342E and D342A cells (Figure 11A,D), while the highest amounts were exhibited by D342N and D342H cells propagated in dim light (Figure 11B,D). In D342N cells, the apparent rate of charge recombination between Q_A^- and Y_Z^{ox} was unusually rapid, exhibiting an inverse rate constant of 13 ± 3 ms (Table 4). By assuming that charge recombination between Q_A^- and P_{680}^+ was not altered by the mutation, these results imply that the Y_Z^{ox}/Y_Z midpoint potential increased significantly

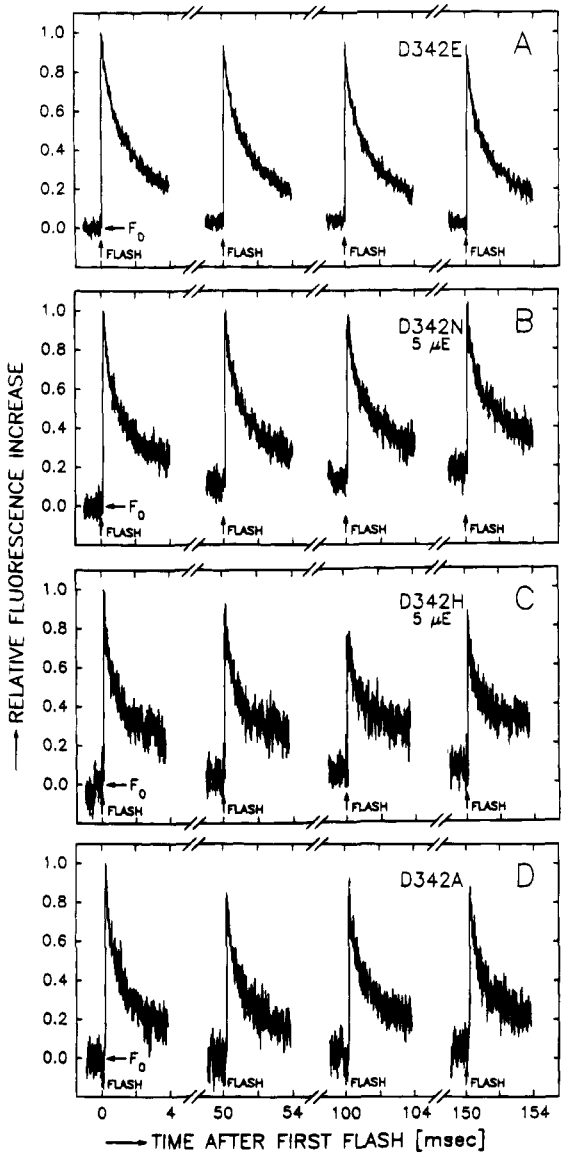

FIGURE 10: Yield of variable chlorophyll *a* fluorescence produced by each of four saturating flashes given at 50 ms intervals to Asp-342 mutant cells. Five milliseconds of data are shown for each flash. (A) D342E; (B) D342N; (C) D342H; (D) D342A. The D342N and D342H cells were propagated in dim light. The conditions were the same as in Figure 1. The maximum $(F - F_0)/F_0$ values measured after the first flash in each series were 0.33 for (A), 0.20 for (B), 0.09 for (C), and 0.13 for (D). Four individual flash series were averaged for (A), five for (B), nine for (C), and eight for (D). The frequency of the monitoring flashes was switched from 1.6 to 100 kHz for 5 ms beginning 1 ms before each flash.

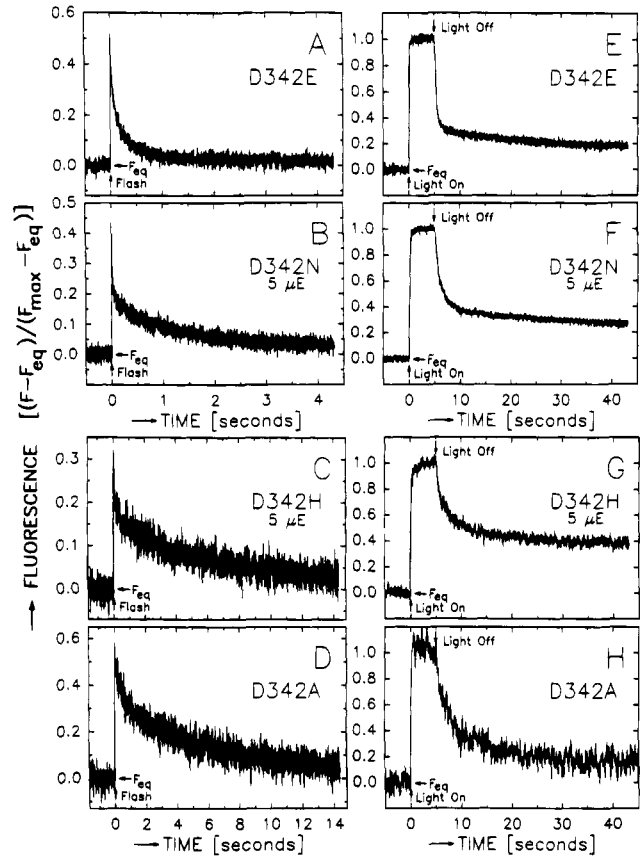

FIGURE 11: Formation and decay of Q_A^- in response to a saturating flash (left panels) or to 5 s of illumination (right panels) given to Asp-342 mutant cells in the presence of DCMU, as measured by changes in the yield of chlorophyll *a* fluorescence: (A, E) D342E; (B, F) D342N; (C, G) D342H; (D, H) D342A. Note the three different time scales employed in this figure. The conditions were the same as in Figure 2. Traces A–D represent the computer averages of 8, 16, 19, and 24 traces, respectively. The monitoring flashes were applied at 1.6 kHz.

in D342N cells, as concluded earlier for a number of His-332 and His-337 mutants (see above) and previously for D170A and D170S cells (Chu et al., 1994a, 1995).

In D342E cells (Figure 11A), one of the two slower components decayed more rapidly, and the other more slowly, than in wild-type* cells. Similar behavior was noted earlier for the H332D and H337R mutants. In D342N cells (Figure 11B), the rates of the two slower decay components were similar to those in wild-type* cells (Table 1), although the slowest decay component was slightly slower. Because the D342E and D342N mutants evolved oxygen at significant rates, the two slower components in these mutants presumably correspond to charge recombination between Q_A^- and altered S_2 states of the Mn cluster. By assuming that charge recombination between Q_A^- and P_{680}^+ was not altered by the mutations, the rates of the slower decay components suggest that the S_2/S_1 midpoint potential in D342E cells increased compared to that in wild-type* cells, while that in D342N cells remained essentially unchanged. In contrast, in D342H and D342A cells (Figure 11C,D), the slowest decaying components exhibited inverse rate constants of 9.2–9.7 s, which are similar to the rates of the slowest components in mutants that lack the extrinsic 33 kDa polypeptide (Chu et al., 1994b). As discussed in relation to the His-332, Glu-333, and His-337 mutants, this slow decay could correspond to charge recombination between Q_A^- and either a single oxidized Mn^{3+} ion or a Mn cluster of unknown nuclearity (Chu et al., 1994b).

When cells were propagated in normal light instead of dim light, the charge recombination kinetics of D342N cells slowed considerably and the relative amounts of the rapidly decaying components in D342N and D342H cells decreased markedly (Table 4). These results show that the D342N and D342H mutants are extremely light-sensitive. Interestingly, the charge recombination kinetics of D342A cells resembled those of mutants that lack the extrinsic 33 kDa polypeptide even when propagated in dim light (*e.g.*, see Figure 11D). In contrast, the charge recombination kinetics of the dark-sensitive D342E cells slowed to some extent in *darkness*, although even after 3–5 h of dark adaptation the kinetics remained faster than in wild-type* cells (not shown).

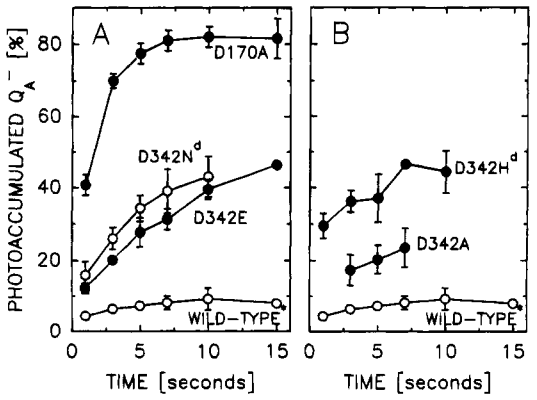

FIGURE 12: Fraction of PSII reaction centers in Asp-342 mutant cells that photoaccumulated Q_A^- after illumination for specific intervals of time (see Figure 11E–H and text): (A) photoaccumulation of Q_A^- in D342E and D342N cells in comparison to wild-type* and D170A cells; (B) photoaccumulation of Q_A^- in D342H and D342A cells in comparison to wild-type* cells. The D342N and D342H cells were propagated in dim light. The wild-type* and D170A data are taken from Chu et al. (1994c) to facilitate comparisons. The conditions were the same as in Figure 3.

Consequently, the *dark* sensitivity of D342E cells was much less than that of H337L cells.

(iii) Photoaccumulation of Q_A^-. To estimate the fractions of PSII reaction centers in the Asp-342 mutants that contain photooxidizable Mn ions, cells were illuminated for 1–15 s in the presence of DCMU. The kinetics of Q_A^- oxidation in D342E, D342N, D342H, and D342A cells after 5 s of illumination are presented in Figure 11E–H. The D342N and D342H cells were propagated in dim light. As with most other mutants (Chu et al., 1994a), the rates of the two *faster* components of Q_A^- oxidation after 5 s of illumination (Figure 11E–H) were roughly similar to the rates of the two *slower* components observed after a single flash (Figure 11A–D, Table 4). The D342N mutant resembled the His-332, H337L, and H337F mutants in that the amplitudes of these components were smaller after a single flash than after 5 s of illumination. As discussed in relation to the His-332, Glu-333, and His-337 mutants, both of these components presumably correspond to charge recombination between Q_A^- and an oxidized form of a Mn cluster (Chu et al., 1994a). The fractions of Q_A^- that *photoaccumulated* during 5 s of illumination were 28% ± 4% in D342E cells (Figure 11E), 34% ± 4% in D342N cells (Figure 11F), 37% ± 7% in D342H cells (Figure 11G), and 20% ± 4% in D342A cells (Figure 11H), compared to 7.2% ± 0.9% in wild-type* cells (Chu et al., 1994a). Figure 12A shows the fraction of Q_A^- that photoaccumulated during 1–15 s of illumination in D342E and D342N cells (the latter propagated in dim light) in comparison to wild-type* and D170A cells. Figure 12B shows the corresponding data for D342H and D342A cells (the former propagated in dim light).

In all four mutants, the rates of Q_A^- photoaccumulation were heterogeneous, with a fraction of PSII reaction centers photoaccumulating Q_A^- during the first second of illumination and other fractions photoaccumulating at slower rates. In D342E and D342N cells (and possibly in D342H and D342A cells), the slower components of Q_A^- photoaccumulation were considerably more rapid than that in wild-type* cells. In D342E cells, the more rapid photoaccumulation rate correlated with the more rapid $Q_A^- \rightarrow S_2$ charge recombination kinetics observed in this mutant. In contrast, the kinetics of $Q_A^- \rightarrow$ Mn charge recombination was unusually rapid in none of the other Asp-342 mutants. Therefore, factors other than electron donation from cytochrome *b*-559 and/or Y_D to P_{680}^+ (Chu et al., 1994a) must contribute to the photoaccumulation of Q_A^- in D342N cells, and possibly in D342H and D342A cells as well. The rapid photoaccumulation of Q_A^- in these mutants may be related to their extreme light sensitivity (see the following).

The data of Figure 12A,B imply that some PSII reaction centers in all of the Asp-342 mutants lack photooxidizable Mn ions *in vivo*. By comparing the extent of Q_A^- photoaccumulation after 3–7 s of illumination with that in wild-type* and D170A cells, we estimate that up to 22–31% of D342E reaction centers, 31–42% of D342N reaction centers, 40–47% of D342H reaction centers, and 17–22% of D342A reaction centers lack photooxidizable Mn ions *in vivo*. These estimates should be considered to be very approximate for reasons enumerated elsewhere (Chu et al., 1994a). Furthermore, in D342N cells (and possibly in D342H and D342A cells), these estimates are probably upper limits because, as noted in the preceding paragraph, additional factors must contribute to the photoaccumulation of Q_A^- in these mutants compared to other cells. Nevertheless, in the D342E and D342H mutants, the estimated fraction of reaction centers that lack photooxidizable Mn ions is in rough agreement with the fraction of Q_A^- that appears to recombine with Y_Z^{ox} after a single saturating flash given in the presence of DCMU (Figure 11A,C). In D342N cells, charge recombination between Q_A^- and Y_Z^{ox} was unusually rapid (Figure 11B, Table 4). Consequently, Q_A^- may compete successfully with Mn for the reduction of Y_Z^{ox} in a significant fraction of reaction centers in this mutant.

(iv) Flash-Induced Increases in Fluorescence Yield. In all of the Asp-342 mutants, the increase in fluorescence yield produced by a saturating flash (relative to F_{max}, see Figure 11A–D) was lower than that in wild-type* cells [the ratio $(F - F_{eq})/(F_{max} - F_{eq})$ was approximately 0.96 in wild-type* cells (Chu et al., 1994a, 1995)]. The lower flash-induced increase was particularly evident in D342H cells (Figure 11C). To determine whether slowed electron transfer from Y_Z to P_{680}^+ contributed to any of the lower flash-induced increases, we measured the increase produced by the first in a series of saturating flashes given in the presence of DCMU and hydroxylamine (Metz et al., 1989; Chu et al., 1994a, 1995). In the D342E and D342N mutants, the ratio $(F_1 - F_0)/(F_{max} - F_0)$ was similar to that in wild-type* cells. [The values were 0.64 ± 0.11 for D342E cells, 0.63 ± 0.05 for D342N cells (propagated in dim light), 0.44 ± 0.04 for D342H cells (propagated in dim light), and 0.46 ± 0.04 for D342A cells, compared to 0.59 ± 0.06 for wild-type* cells (Chu et al., 1994b).] The value for D342N cells did not change when these cells were propagated in normal light. These data imply that slowed electron transfer from Y_Z to P_{680}^+ *may* contribute to the lower flash-induced increases in fluorescence yield observed in the *absence* of hydroxylamine only in D342H and D342A cells. In D342E and D342N cells, the lower flash-induced increases may be caused by the higher equilibrium concentrations of P_{680}^+ present because of the apparent shifts in the S_2/S_1 and Y_Z^{ox}/Y_Z midpoint potentials in D342E and D342N cells, respectively (Chu et al., 1994a).

(v) Requirement for Ca^{2+} Ions. The Ca^{2+} requirements of D342E and D342N cells were investigated. As stated

earlier, D342E cells did not grow photoautotrophically in the absence of Ca^{2+} ions. When propagated *photoheterotrophically* in medium containing Na^+ substituted for Ca^{2+}, neither D342E nor D342N cells evolved oxygen and both exhibited only small increases in fluorescence yield when subjected to saturating flashes in the presence of DCMU and hydroxylamine (not shown). In this respect, D342E and D342N cells resembled the His-332, Glu-333, and His-337 mutants (see above) and D59N and D61A cells (Chu et al., 1995): electron transfer from Y_Z to P_{680}^+ appeared to slow dramatically when the cells were propagated in the absence of Ca^{2+} ions.

(C) Light Sensitivity and Photoinhibition. The lower apparent PSII content and slower charge recombination kinetics of D342N cells, and the diminished amounts of rapid charge recombination kinetics in D342N and D342H cells propagated in normal rather than dim light, show that these mutants are extremely light-sensitive. In this respect, these Asp-342 mutants resemble the Glu-333 mutants, the four light-sensitive His-332 mutants, and the three light-sensitive His-337 mutants. Because a similar light sensitivity is not observed in mutants that lack photooxidizable Mn ions, we have proposed that the altered or partly assembled Mn clusters in the light-sensitive His-332, Glu-333, and His-337 mutants prematurely oxidize a water-derived ligand and give off toxic, activated oxygen species such as hydrogen peroxide (see above). We propose that a similar mechanism operates in D342N and D342H cells. Furthermore, the rapid photoaccumulation of Q_A^- in D342N cells suggests that the postulated premature oxidation of a water-derived ligand may occur in the altered S_2 state of this mutant, as proposed earlier for the mutants E333H, E333N, H337E, and H337D.

(D) Role of Asp-342 in Posttranslational Processing. Posttranslational cleavage of the carboxy-terminal extension of the D1 polypeptide's precursor form has been reported to require the negative charge of Asp-342 (Taguchi et al., 1993). This conclusion was based on enzymatic assays conducted with synthetic oligopeptides *in vitro*. Enzymatic cleavage of a 16-amino acid oligopeptide was practically eliminated when the Asp residue corresponding to Asp-342 was replaced with Asn (Taguchi et al., 1993). To test the possibility that the characteristics of our Asp-342 mutants are influenced by an inability to posttranslationally cleave the D1 polypeptide's carboxy-terminal extension, all four mutants were also constructed as double mutants that contained a stop codon in place of Ser-345. In these mutants, the D1 polypeptide is expected to be synthesized without its carboxy-terminal extension (Nixon et al., 1992). The growth, oxygen-evolving activities, apparent PSII contents, and fluorescence characteristics of the D342E, D342N, D342H, and D342A mutants constructed in the presence of the Ser-345 → stop mutation were indistinguishable from those of the original mutants (data not shown). Therefore, we conclude that the negative charge of Asp-342 is *not* essential for posttranslational processing of the D1 polypeptide *in vivo* and that the characteristics of our Asp-342 mutants are *not* influenced by the failure to process the carboxy-terminal extension. Indeed, Nixon, Diner, and coworkers have shown that posttranslational processing occurs efficiently in the D342V mutant of *Synechocystis* 6803 (Nixon et al., 1992). A slower *rate* of processing in the absence of a negative charge at Asp-342 might account for the inability of the processing enzyme to cleave the Asp → Asn oligopeptide efficiently *in vitro*, however (Taguchi et al., 1993).

(E) Involvement in Mn Binding. All of the Asp-342 mutants contain some PSII reaction centers that lack photooxidizable Mn ions (Figure 12A,B). These results show that Asp-342 influences the assembly and/or stability of the Mn cluster. However, because most of the reaction centers in these mutants appear to *contain* photooxidizable Mn ions, Asp-342, like His-332, Glu-333, and His-337, probably does not ligate the first Mn^{2+} ion that binds during assembly of the Mn cluster. Indeed, in preliminary accounts, Nixon, Diner, and co-workers reported that the high-affinity Mn^{2+} binding site first occupied is unperturbed in Asp-342 mutants (Diner et al., 1991; Nixon et al., 1992; Nixon & Diner, 1994; Tang et al., 1994b). Because D342N cells evolved oxygen at significant rates when propagated in dim light, and because Asn apparently can replace His as a ligand to Fe in cytochrome *bo* ubiquinol oxidase from *Escherichia coli* (Calhoun et al., 1993), one possibility is that Asp-342 ligates a Mn ion that binds subsequent to the first. If so, His may be unable to effectively substitute as a ligand for steric reasons. However, if Asp-342 ligates Mn, it is curious that the apparent S_2/S_1 midpoint potential of D342N cells resembles that of wild-type* cells more closely than does the apparent S_2/S_1 midpoint potential of D342E cells. Perhaps the larger size of Glu perturbs the Mn ligation environment. In staphylococcal nuclease, Asp-21 ligates the Ca^{2+} ion as a monodentate ligand, and Glu-43 ligates via an immobilized water molecule. In the D21E mutant, the larger Glu residue ligates as a *bidentate* ligand and displaces the Ca^{2+} ion 1.5 Å from its location in the wild-type structure, resulting in direct ligation by Glu-43 (Libson et al., 1994; Weber et al., 1994).

(F) Involvement in Ca^{2+} Binding. An alternate possibility is that Asp-342 binds a Ca^{2+} ion. The inability of D342E cells to grow photoautotrophically when Ca^{2+} was replaced by Sr^{2+}, Mg^{2+}, or Na^+ and the apparent slowing of electron transfer from Y_Z to P_{680}^+ when D342E or D342N cells were propagated photoheterotrophically in the absence of Ca^{2+} ions demonstrate that the affinity of PSII for Ca^{2+} in these mutants is too low to utilize the quantities of adventitious Ca^{2+} present in our Ca^{2+}-depleted growth media. If Asp-342 ligates a Ca^{2+} ion in PSII, then weakened binding of Ca^{2+} in D342N reaction centers would not be unexpected [*e.g.*, see Maune et al. (1992) and Babu et al. (1992)]. Similarly, weakened binding of Ca^{2+} in D342E reaction centers would not be without precedent (Babu et al., 1992). However, if Asp-59 and Asp-61 also ligate a Ca^{2+} ion in PSII (Chu et al., 1995), then either the carboxy-terminal region of the D1 polypeptide is located in close proximity to Asp-59 and Asp-61 or there is more than one Ca^{2+} ion in the PSII core [see the discussion of the Asp-59 and Asp-61 mutants in Chu et al. (1995)]. If Asp-342 ligates a Ca^{2+} ion, then either the influence of this residue on the assembly and/or stability of the Mn cluster is indirect or this residue serves as a bridging ligand between Ca^{2+} and Mn, as in concanavalin A (Hardman et al., 1982) [also see Chakrabarti (1990a)].

(G) A Possible Structural Role. A third possibility is that Asp-342 performs an important structural role in PSII that is partly satisfied by the carboxylate moiety of Glu, but much less effectively by Asn and His and not at all by Ala. For example, Asp-342 may help orient a His residue that ligates

the Mn cluster. As noted earlier, the $\delta 1$ (or π) nitrogen of a metal-ligating histidine residue typically forms a hydrogen bond with a peptide carbonyl group or a carboxylate residue (Chakrabarti, 1990b). This hydrogen bond helps orient the His residue, and its strength modulates the strength of the His−metal interaction (Christianson & Alexander, 1989; Chakrabarti, 1990b; Goodin & McRee, 1993). In cytochrome *c* peroxidase, Asp-235 and His-175 form such an interaction, with His-175 ligating the heme Fe atom with its $\epsilon 2$ (or τ) nitrogen. The D235E mutation introduces only slight structural perturbations into the enzyme active site, but significantly weakens the strength of the carboxylate−histidine hydrogen bond. This weakened hydrogen bond, in turn, weakens the His−Fe interaction, increasing the heme midpoint potential by approximately 70 mV (Goodin & McRee, 1993). If Asp-342 similarly orients a His ligand to the Mn cluster (*e.g.*, His-190, His-332, or His-337), the apparent increase in the S_2/S_1 midpoint potential in D342E cells would not be unprecedented. Spectroscopic characterization of isolated PSII particles will be required to clarify the role of Asp-342 in PSII function.

SUMMARY AND CONCLUSIONS

Of all of the conserved carboxylate and histidine residues in the carboxy-terminal domain of the D1 polypeptide, only His-332, Glu-333, His-337, and Asp-342 exert any significant influence on oxygen evolution under the conditions of our experiments. Of these residues, His-332, Glu-333, and His-337 may ligate Mn, while Asp-342 may ligate Mn, Ca^{2+}, or both. However, alternate possibilities are also likely. For example, either His-332 or His-337 may serve as a crucial hydrogen bond donor rather than as a ligand to Mn, Glu-333 may participate in a crucial network of hydrogen bonds, and Asp-342 may help position a histidine residue that ligates Mn, thereby modulating the His−metal interaction. The binding of Ca^{2+} is influenced by His-332, Glu-333, and His-337, but none of these residues is likely to ligate Ca^{2+}. If His-332 ligates Mn, then, because Gln and Ser are the most effective functional substitutes, His-332 is unlikely to become oxidized or recruited as a bridging ligand during the catalytic cycle. Also, its influence on the S_2/S_1 midpoint potential would be complex. If Glu-333 ligates Mn, then, because Gln is the most effective functional substitute, Glu-333 presumably would be a monodentate ligand. Also, it would have little apparent influence on the S_2/S_1 midpoint potential. If His-337 ligates Mn, then, because Arg and Gln are the most effective functional substitutes (other than Phe), His-337 is also unlikely to become oxidized or recruited as a bridging ligand during the catalytic cycle. The Phe and Leu substitutions probably cause structural perturbations that permit the missing imidazole moiety to be replaced by another residue, a peptide carbonyl oxygen, or a water molecule. If Asp-342 ligates Mn, then, because Asn is a partly functional substitute when the cells are propagated in dim light, Asp-342 presumably would ligate with only a single oxygen atom. Also, it too would have little apparent influence on the S_2/S_1 midpoint potential. If His-332, Glu-333, His-337, and Asp-342 *all* ligate the Mn cluster, in addition to Asp-170 and His-190 [see the preceding paper in this issue (Chu et al., 1995)] and the carboxy-terminus of Ala-344 (Nixon et al., 1992), then at least 5 of the 14 coordination positions on the Mn cluster that are not occupied by μ_2-oxo bridging ligands in current models (Yachandra et al., 1993; DeRose et al., 1994) are occupied by a combination of peptide carbonyl oxygens, water molecules, conserved D1 residues other than Asp, Glu, His, and Tyr, and amino acid residues from polypeptides other than D1.

Numerous His-332, Glu-333, His-337, and Asp-342 mutants are extremely light-sensitive.[3] When propagated in normal light (50−60 μE m^{-2} s^{-1}), the apparent PSII contents and fluorescence properties of these mutants resemble those of mutants that lack the extrinsic 33 kDa polypeptide. Because Asp-170 mutants that lack photooxidizable Mn ions do not exhibit similar light sensitivity, we propose that the perturbed or partly assembled Mn clusters in the light-sensitive mutants release toxic, activated oxygen species (*e.g.*, hydrogen peroxide) by prematurely oxidizing a water-derived ligand during the catalytic cycle. A similar mechanism of light-induced damage has been postulated to occur in Cl^--depleted PSII membranes and involves the rapid loss of 1−2 Mn ions from PSII (Jegerschöld et al., 1992). Perhaps the similarity of the fluorescence properties of our light-damaged mutants and mutants that lack the extrinsic 33 kDa polypeptide is caused by weaker binding of the extrinsic 33 kDa polypeptide in the absence of intact Mn clusters (Miyao & Murata, 1989; Kavelaki & Ghanotakis, 1991). The fluorescence properties of some mutants (*e.g.*, E333Y, H337V, H337Y, and D342A) resemble those of mutants without the extrinsic 33 kDa polypeptide even when propagated in dim light. These observations suggest that these mutants may be light-damaged, even when propagated at low light intensities (*e.g.*, at 5−6 μE m^{-2} s^{-1}). Alternatively, structural perturbations caused by these mutations may interfere with the proper binding of the extrinsic 33 kDa polypeptide, suggesting that this polypeptide may interact with the carboxy-terminal domain of the D1 polypeptide, as discussed previously (Chu et al., 1994b).

The mutations H332N, H332D, H332E, H332K, H337F, H337L, and D342N appear to significantly perturb the Y_Z^{ox}/Y_Z midpoint potential, as indicated by the unusually rapid charge recombination between Q_A^- and Y_Z^{ox} in these mutants. These results suggest that the carboxy-terminal domain may be in close proximity to the base of the C helix of the D1 polypeptide, as proposed by Nixon, Diner, and co-workers (Diner et al., 1991). Long-range mutation-induced structural alterations cannot be excluded, however.

Most of the mutants described in this paper exhibit slowed electron transfer from Q_A^- to Q_B. A similar slowing of this electron-transfer step was noted previously in several Glu-65, Asp-170, and Glu-189 mutants and in D61A cells (Chu et al., 1994a, 1995). These observations are a further indication that alterations in the donor side of PSII may also alter properties of the acceptor side [*e.g.*, see Krieger and Weis (1992), Krieger et al. (1993), Johnson et al. (1995), and the discussion in Chu et al. (1994a)].

[3] We previously reported that numerous site-directed mutants from the carboxy-terminal domain of the D1 polypeptide exhibit fluorescence properties that resemble those of cells that lack the extrinsic 33 kDa polypeptide. We suggested that the extrinsic 33 kDa polypeptide binds weakly or improperly to PSII in these mutants and further suggested that this polypeptide interacts with the carboxy-terminal region of the D1 polypeptide (Chu et al., 1994b). Since that time, we have determined that most of the mutants considered are extremely light-sensitive and exhibit different fluorescence properties when propagated in dim light. In contrast, the fluorescence properties of cells that *lack* the extrinsic 33 kDa polypeptide (Chu et al., 1994b) are essentially the same whether propagated in normal light or dim light (not shown).

Finally, the negative charge of Asp-342 is not essential for posttranslational processing of the D1 polypeptide's precursor form *in vivo*.

The results presented in this and the accompanying paper (Chu et al., 1995) will guide future studies of isolated mutant PSII particles to residues of particular interest in terms of Mn or Ca^{2+} ligation or other aspects of PSII function and to mutants that contain the most stable or most efficiently assembled Mn clusters *in vivo*.

ADDED IN PROOF

We recently found that DCMU protects against light-induced damage in those mutants that are sensitive to light. The apparent PSII contents of light-sensitive cells are higher when propagated in the presence of 10 μM DCMU in *normal* light than when propagated in the absence of DCMU in *dim* light. In most cases, the apparent PSII contents are similar to that of wild-type* cells. After washing, the oxygen evolution and fluorescence properties of wild-type* cells are the same whether propagated in the presence or absence of 10 μM DCMU.

ACKNOWLEDGMENT

We thank G. T. Babcock, B. A. Barry, T. M. Bricker, R. D. Britt, G. W. Brudvig, R. B. Burnap, B. A. Diner, J. M. Erickson, W. D. Frasch, D. F. Ghanotakis, P. J. Nixon, A. W. Rutherford, R. T. Sayre, M. Seibert, and C. F. Yocum for many stimulating discussions during the course of this study. We are particularly indebted to P. J. Nixon and B. A. Diner for sharing the results of their site-directed mutagenesis studies prior to publication. Finally, we thank G. T. Babcock, T. Bricker, B. A. Diner, M. Seibert, W. F. J. Vermaas, and the reviewers for helpful comments on the manuscript and H. K. Suruki for assistance with some of the H337Q cultures.

REFERENCES

Ananyev, G., Wydrzynski, T., Renger, G., & Klimov, V. V. (1992) *Biochim. Biophys. Acta 1100*, 303−311.

Aro, E.-M., Virgin, I., & Andersson, B. (1993) *Biochim. Biophys. Acta 1143*, 113−134.

Babu, A., Su, H., Ryu, Y., & Gulati, J. (1992) *J. Biol. Chem. 267*, 15469−15474.

Barrick, D. (1994) *Biochemistry 33*, 6546−6554.

Blubaugh, D. J., Atamian, M., Babcock, G. T., Golbeck, J. H., & Cheniae, G. M. (1991) *Biochemistry 30*, 7586−7597.

Boerner, R. J., Nguyen, A. P., Barry, B. A., & Debus, R. J. (1992) *Biochemistry 31*, 6660−6672.

Bouges-Bocquet, B. (1980) *Biochim. Biophys. Acta 594*, 85−103.

Boussac, A., Zimmermann, J.-L., Rutherford, A. W., & Lavergne, J. (1990) *Nature 347*, 303−306.

Boussac, A., Sétif, P., & Rutherford, A. W. (1992) *Biochemistry 31*, 1224−1234.

Bradley, R. L., Long, K. M., & Frasch, W. D. (1991) *FEBS Lett. 286*, 209−213.

Brudvig, G. W., & Crabtree, R. H. (1989) *Prog. Inorg. Chem. 37*, 99−142.

Burnap, R. L., Shen, J.-R., Jursinic, P. A., Inoue, Y., & Sherman, L. A. (1992) *Biochemistry 31*, 7404−7410.

Buser, C. A. (1993) *Electron-Transfer Reactions in Photosystem II*, Ph.D. Dissertation, Yale University, New Haven, CT.

Buser, C. A., Thompson, L. K., Diner, B. A., & Brudvig, G. W. (1990) *Biochemistry 29*, 8977−8985.

Buser, C. A., Diner, B. A., & Brudvig, G. W. (1992) *Biochemistry 31*, 11449−11459.

Calhoun, M. W., Lemieux, L. J., Thomas, J. W., Hill, J. J., Chepuri Goswitz, V., Alben, J. O., & Gennis, R. B. (1993) *Biochemistry 32*, 13254−13261.

Chakrabarti, P. (1990a) *Protein Eng. 4*, 49−56.

Chakrabarti, P. (1990b) *Protein Eng. 4*, 57−63.

Choudhury, K., Sundaramoorthy, M., Mauro, J. M., & Poulos, T. L. (1992) *J. Biol. Chem. 267*, 25656−25659.

Choudhury, K., Sundaramoorthy, M., Hickman, A., Yonetani, T., Woehl, E., Dunn, M. F., & Poulos, T. L. (1994) *J. Biol. Chem. 269*, 20239−20249.

Christianson, D. W., & Alexander, R. S. (1989) *J. Am. Chem. Soc. 111*, 6412−6419.

Chu, H.-A., Nguyen, A. P., & Debus, R. J. (1994a) *Biochemistry 33*, 6137−6149.

Chu, H.-A., Nguyen, A. P., & Debus, R. J. (1994b) *Biochemistry 33*, 6150−6157.

Chu, H.-A., Nguyen, A. P., & Debus, R. J. (1995) *Biochemistry 34*, 5839−5858.

Debus, R. J. (1992) *Biochim. Biophys. Acta 1102*, 269−352.

den Blaauwen, T., & Canters, G. W. (1993) *J. Am. Chem. Soc. 115*, 1121−1129.

DePillis, G. D., Decatur, S. M., Barrick, D., & Boxer, S. G. (1994) *J. Am. Chem. Soc. 116*, 6981−6982.

DeRose, V. J., Mukerji, I., Latimer, M. J., Yachandra, V. K., Sauer, K., & Klein, M. P. (1994) *J. Am. Chem. Soc. 116*, 5239−5249.

Diner, B. A., Nixon, P. J., & Farchaus, J. W. (1991) *Curr. Opin. Struct. Biol. 1*, 546−554.

Eckert, H.-J., Geiken, B., Bernarding, J., Napiwotzki, A., Eichler, H.-J., & Renger, G. (1991) *Photosynth. Res. 27*, 97−108.

Ferrer, J. C., Guillemette, J. G., Bogumil, R., Inglis, S. C., Smith, M., & Mauk, A. G. (1993) *J. Am. Chem. Soc. 115*, 7507−7508.

Fine, P. L., & Frasch, W. D. (1992) *Biochemistry 31*, 12204−12210.

Garcia, L. L., Fredericks, Z., Sorrell, T. N., & Pielack, G. J. (1992) *New J. Chem. 16*, 629−632.

Goodin, D. B., & McRee, D. E. (1993) *Biochemistry 32*, 3313−3324.

Haining, R. L., & McFadden, B. A. (1994) *Photosynth. Res. 41*, 349−356.

Hampsey, D. M., Das, G., & Sherman, F. (1986) *J. Biol. Chem. 261*, 3259−3271.

Hardman, K. D., Agarwal, R. C., & Freiser, M. J. (1982) *J. Mol. Biol. 157*, 69−86.

Hillier, W., & Wydrzynski, T. (1993) *Photosynth. Res. 38*, 417−423.

Howell, E. E., Villafranca, J. E., Warren, M. S., Oatley, S. J., & Kraut, J. (1986) *Science 231*, 1123−1128.

Jegerschöld, C., & Styring, S. (1991) *FEBS Lett. 280*, 87−90.

Jegerschöld, C., Virgin, I., & Styring, S. (1990) *Biochemistry 29*, 6179−6186.

Jegerschöld, C., Ågren, H., & Styring, S. (1992) in *Research in Photosynthesis* (Murata, N., Ed.) Vol. II, pp 421−424, Kluwer Academic Publishers, Dordrecht, The Netherlands.

Johnson, G., Rutherford, A. W., & Krieger, A. (1995) *Biochim. Biophys. Acta* (in press).

Joseph-McCarthy, D., Rost, L. E., Komives, E. A., & Petsko, G. A. (1994) *Biochemistry 33*, 2824−2829.

Kavelaki, K., & Ghanotakis, D. F. (1991) *Photosynth. Res. 29*, 149−155.

Kim, Y., Misna, D., Monzingo, A. F., Ready, M. P., Frankel, A., & Robertus, J. D. (1992) *Biochemistry 31*, 3294−3296.

Klimov, V. V., Ananyev, G., Zastryzhnaya, O., Wydrzynski, T., & Renger, G. (1993) *Photosynth. Res. 38*, 409−416.

Krieger, A., & Weis, E. (1992) *Photosynthetica 27*, 89−98.

Krieger, A., Weis, E., & Demeter, S. (1993) *Biochim. Biophys. Acta 1144*, 411−418.

Libson, A. M., Gittis, A. G., & Lattman, E. E. (1994) *Biochemistry 33*, 8007−8016.

Loll, P. J., & Lattman, E. E. (1990) *Biochemistry 29*, 6866−6873.

Martín, A. E., Burgess, B. K., Stout, C. D., Cash, V. L., Dean, D. R., Jensen, G. M., & Stephens, P. M. (1990) *Proc. Natl. Acad. Sci. U.S.A. 87*, 598−602.

Maune, J. F., Klee, C. B., & Beckingham, K. (1992) *J. Biol. Chem. 267*, 5286−5295.

McPhalen, C. A., Strynadka, N. C. J., & James, M. N. G. (1991) *Adv. Protein Chem. 42*, 77−144.

Metz, J. G., Nixon, P. J., Rögner, M., Brudvig, G. W., & Diner, B. A. (1989) *Biochemistry 28*, 6960−6969.
Miller, A.-F., & Brudvig, G. W. (1989) *Biochemistry 28*, 8181−8190.
Miyao, M. (1994) *Biochemistry 33*, 9722−9730.
Miyao, M., & Murata, N. (1989) *Biochim. Biophys. Acta 977*, 315−321.
Mizrahi, V., Brooksbank, R. L., & Nkabinde, N. C. (1994) *J. Biol. Chem. 269*, 19245−19249.
Nixon, P. J., & Diner, B. A. (1992) *Biochemistry 31*, 942−948.
Nixon, P. J., & Diner, B. A. (1994) *Biochem. Soc. Trans. 22*, 338−343.
Nixon, P. J., Trost, J. T., & Diner, B. A. (1992) *Biochemistry 31*, 10859−10871.
Pecoraro, V. L. (1988) *Photochem. Photobiol. 48*, 249−264.
Philbrick, J. B., Diner, B. A., & Zilinskas, B. A. (1991) *J. Biol. Chem. 266*, 13370−13376.
Prášil, O., Adir, N., & Ohad, I. (1992) in *The Photosystems: Structure, Function and Molecular Biology* (Barber, J., Ed.) pp 295−348, Elsevier Science Publishers, B.V., Amsterdam.
Quillin, M. L., Arduini, R. M., Olson, J. S., & Phillips, G. N., Jr. (1993) *J. Mol. Biol. 234*, 140−155.
Renger, G. (1993) *Photosynth. Res. 38*, 229−247.
Richardson, J. S., & Richardson, D. C. (1989) in *Prediction of Protein Structure and the Principles of Protein Conformation* (Fasman, G. D., Ed.) pp 1−98, Plenum Press, New York.
Rova, M., Franzén, L.-G., Fredriksson, P.-O., & Styring, S. (1994) *Photosynth. Res. 39*, 75−83.
Rutherford, A. W. (1989) *Trends Biochem. Sci. 14*, 227−232.
Rutherford, A. W., Zimmermann, J.-L., & Boussac, A. (1992) in *The Photosystems: Structure, Function and Molecular Biology* (Barber, J., Ed.) pp 179−229, Elsevier Science Publishers, B.V., Amsterdam.
Satoh, Ka., & Katoh, S. (1985) *FEBS Lett. 190*, 199−203.
Sorrell, T. N., Martin, P. K., & Bowden, E. F. (1989) *J. Am. Chem. Soc. 111*, 766−767.
Stone, C. L., Hurley, T. D., Amzel, L. M., Dunn, M. F., & Bosron, W. F. (1993) in *Enzymology and Molecular Biology of Carbonyl Metabolism 4* (Weiner, H., Ed.) pp 429−437, Plenum Press, New York.
Sundaramoorthy, M., Choudhury, K., Edwards, S. L., & Poulos, T. L. (1992) *J. Am. Chem. Soc. 113*, 7755−7757.
Svensson, B., Vass, I., & Styring, S. (1991) *Z. Naturforsch. 46c*, 765−776.
Taguchi, F., Yamamoto, Y., Inagaki, N., & Satoh, Ki. (1993) *FEBS Lett. 326*, 227−231.
Tamura, N., & Cheniae, G. M. (1988) in *Light-Energy Transduction in Photosynthesis: Higher Plant and Bacterial Models* (Stevens, S. E., Jr., & Bryant, D. A., Eds.) pp 227−242, American Society of Plant Physiologists, Rockville, MD.
Tamura, N., Inoue, Y., & Cheniae, G. M. (1989) *Biochim. Biophys. Acta 976*, 173−181.
Tang, X.-S., Diner, B. A., Larsen, B. S., Gilchrist, M. L., Jr., Lorigan, G. A., & Britt, R. D. (1994a) *Proc. Natl. Acad. Sci. U.S.A. 91*, 704−708.
Tang, X.-S., Nixon, P. J., Britt, R. D., & Diner, B. A. (1994b) *Photochem. Photobiol. 59*, 82S-83S.
Thompson, L. K., Blaylock, R., Sturtevant, J. M., & Brudvig, G. W. (1989) *Biochemistry 28*, 6686−6695.
Ubbink, M., Campos, A. P., Teixeira, M., Hunt, N. I., Hill, H. A. O., & Canters, G. W. (1994) *Biochemistry 33*, 10051−10059.
Vass, I., & Styring, S. (1991) *Biochemistry 30*, 830−839.
Vass, I., Cook, K. M., Deák, Z., Mayes, S. R., & Barber, J. (1992) *Biochim. Biophys. Acta 1102*, 195−201.
Weber, D. J., Libson, A. M., Gittis, A. G., Lebowitz, M. S., & Mildvan, A. S. (1994) *Biochemistry 33*, 8017−8028.
Wieghardt, K. (1989) *Angew. Chem., Int. Ed. Engl. 28*, 1153−1172.
Wydrzynski, T., Ångström, J., & Vänngård, T. (1989) *Biochim. Biophys. Acta 973*, 23−28.
Yachandra, V. K., DeRose, V. J., Latimer, M. J., Mukerji, I., Sauer, K., & Klein, M. P. (1993) *Science 260*, 675−679.
Yerkes, C. T., Babcock, G. T., & Crofts, A. R. (1983) *FEBS Lett. 158*, 359−363.

BI942562Z